JOURNAL OF GEOPHYSICAL RESEARCH, VOL. 104, NO. C9, PAGES 21,151–21,170, SEPTEMBER 15, 1999

On the circulation in the upper layer of the western equatorial Atlantic

B. Bourlès, Y. Gouriou and R. Chuchla

Centre IRD de Bretagne, Plouzané, France

Abstract. Hydrographic observations of pressure, temperature, salinity, dissolved oxygen, and shipboard acoustic Doppler current profiler measurements are used to study the upper layer circulation in the western equatorial Atlantic Ocean, limited to the region bounded by the 10°S and 14°N latitudes between the longitudes 30°W and 52°W. Data were obtained during four World Ocean Circulation Experiment cruises, carried out in January-March 1993, January-March 1994, September-October 1995, and April-May 1996. In the upper layer, the continuity of the northwestward flowing North Brazil Current along the American continent toward the Caribbean Sea is confirmed in boreal spring. Furthermore, part of the North Brazil Current also continues northwestward in the subthermocline layer during short periods in boreal spring, contrary to previous estimates. The North Equatorial Countercurrent (NECC) is present in boreal spring west of 40°W, fed with water of Northern Hemisphere origin only. The southeastward flowing current observed at 3°N-44°W is fed by the North Brazil Current retroflection and by a cyclonic recirculation of the southern edge of the North Equatorial Current. The upper layer of this current, at 3°N-44°W, feeds the Equatorial Undercurrent (EUC) and the NECC, when its subthermocline layer feeds the EUC and the North Equatorial Undercurrent. Near-surface eastward flow is present above the EUC during all cruises, yielding to a strong increase of the eastward warm water transport.

1. Introduction

The western tropical Atlantic is an area of crucial interest with regard to the thermohaline circulation and associated mass, heat, and salt transports. There, the strong North Brazil Current (NBC) transports warm upper ocean waters toward the Northern Hemisphere [*Metcalf and Stalcup*, 1967; *Metcalf*, 1968]. It thus contributes to balance the southward flow of cold North Atlantic Deep Water [*Fine and Molinari*, 1988] and to close the meridional overturning cell of the global thermohaline circulation [*Gordon*, 1986]. *Schmitz and McCartney* [1993] and *Schmitz* [1995] estimate this overturning cell to an amount ranging between 13 and 17 Sv ($1\ Sv = 10^6\ m^3\ s^{-1}$). *Wilson and Johns* [1997] estimate that 8 Sv of waters of southern origin contribute to the Atlantic thermohaline cell through the southern passages of the Caribbean Sea, via a northwestward route along the American coast. In the Florida Current, *Schmitz and Richardson* [1991] and *Schmitz* [1995] estimate the transport of waters of southern origin as 13-14 Sv for temperature warmer than 7°C. Recent studies suggest that water of South Atlantic origin must join the Florida Current after being carried eastward by the NBC retroflection and then westward in the North Equatorial Current (NEC) [*Mayer and Weisberg*, 1993; *Wilson and Johns*, 1997]. *Wilson and Johns* [1997] also evoke the possibility that part of the South Atlantic water does not transit toward the northern high latitudes through the Florida Current.

Paper number 1999JC900058
0148-0227/99/1999JC900058$09:00

da Silveira et al. [1994] have shown that, between 10°S and 5°S, the velocity core of the NBC is centered at about 100-200 m depth, instead of at the surface, as previously thought. *Stramma et al.* [1995] define this undercurrent as the North Brazil Undercurrent (NBUC). *Schott et al.* [1995] show that the NBC originates in the overriding of the South Equatorial Current (SEC) on the NBUC, north and west of 5°S-35°W, after passing the Cape San Roque. Then, the NBC exhibits a very complex behavior and feeds surface and subsurface eastward flows at different depths and different latitudes. Namely, from south to north, it feeds the South Equatorial Undercurrent (SEUC), the Equatorial Undercurrent (EUC), the North Equatorial Undercurrent (NEUC), and the North Equatorial Countercurrent (NECC) [*Metcalf and Stalcup*, 1967; *Cochrane et al.*, 1979; *Stramma and Schott*, 1996]. The NECC, NEUC, and EUC are, however, also fed with waters of Northern Hemisphere origin, through a cyclonic recirculation of the NEC taking place north of the NBC retroflection loop and through a coastally trapped subsurface current, the Western Boundary Undercurrent (WBUC). The existence of this current was suggested in the measurements of *Flagg et al.* [1986] and *Johns et al.* [1990] and confirmed by more recent observations [*Colin and Bourlès*, 1994; *Wilson et al.*, 1994; *Bourlès et al.*, 1999]. The quantification of mean and seasonal transports and water mass contents of the different currents is made very difficult owing to a large spatial and time variability encountered in this region and to eddies that detach from the NBC retroflection from boreal summer to winter [*Johns et al.*, 1990; *Didden and Schott*, 1993; *Schott et al.*, 1993; *Colin et al.*, 1994; *Wilson et al.*, 1994; *Johns et al.*, 1998]. Thus, for example, while *Wilson et al.* [1994] and *Bourlès et al.* [1999] show that the NBC retroflection is total from June to January, the continuity

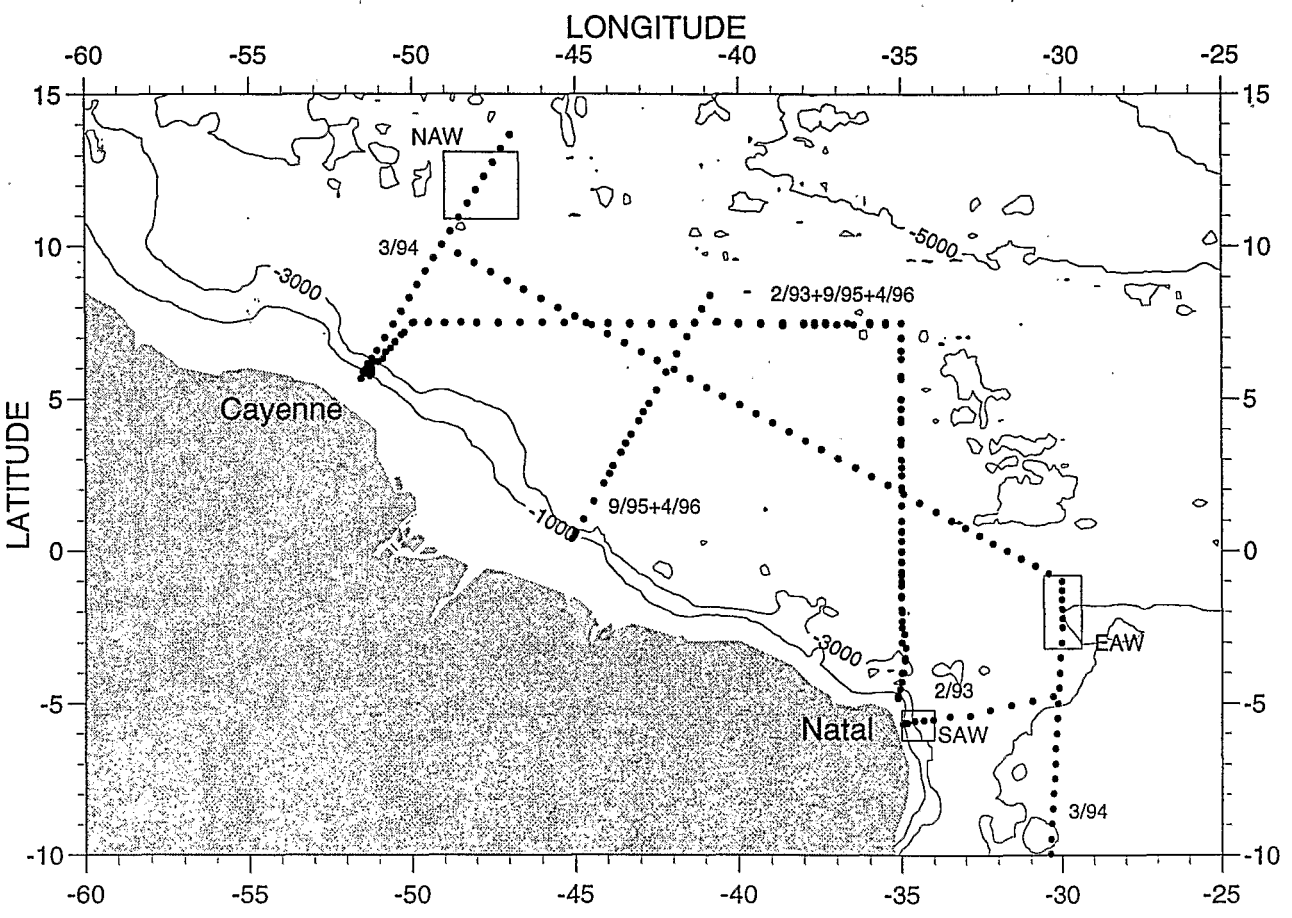

Figure 1. Section map of the studied region. Cruise tracks are identified by month/year. Profiles used to define the three water mass classes (southern tropical Atlantic water (SAW), eastern tropical Atlantic water (EAW), and northern tropical Atlantic water (NAW); see text for further explanation) are marked by boxes.

of the NBC along the boundary in boreal spring, suggested by *Schott et al.* [1995, 1998] and *Johns et al.* [1998], is still not proven.

We present here additional synoptic descriptions of the upper layer currents and water mass distributions from four recent surveys carried out as part of the World Ocean Circulation Experiment (WOCE) Hydrographic Programme in the western tropical Atlantic. The cruises and available data are described first. Then, we explain the transport calculation, after summarizing the water masses present in the region and the main currents. Currents and water mass pathways are analyzed in the NBC retroflection zone and off French Guiana. As a conclusion, the results that improve our knowledge of some main aspects of the circulation are discussed.

2. Data

The data used in this study were collected in 1993, 1994, 1995, and 1996 during two Circulation Thermohaline programme in the south and equatorial Atlantic (CITHER) and Etude du Transport Atlantique Méridien dans le Bassin Ouest équatorial (ETAMBOT) cruises. The CITHER 1 cruise was carried out on R/V *L'Atalante* between January 2 and March 19, 1993; two basin-wide zonal sections were realized at latitudes 7°30'N and 4°30'S, complemented by two meridional sections at 35°W and 4°W between these latitudes. The CITHER 2 cruise was carried out on R/V *Maurice Ewing* between January 4 and March 21, 1994; one meridional section was realized from 50°S to 14°N parallel to the South America coastline, along with three sections perpendicular to the coast. The ETAMBOT 1 cruise was carried out on R/V *Le Noroit* between September 9 and October 10, 1995, and the ETAMBOT 2 cruise occurred on R/V *Edwin Link* between April 4 and May 16, 1996. The two ETAMBOT track lines repeat the 35°W and the western part of the 7°30'N CITHER 1 sections. Furthermore, a third section (hereafter referred to as the Ceara section) was carried out perpendicular to the Brazil coast, between 0°,45°W and 8°20'N,41°W. The section located off French Guiana is common to every cruise. For each cruise, the station spacing is about 30 nautical miles (55.6 km) and reduced near the equator and the coasts. The area considered in this study is limited to the region bounded by the 10°S and 14°N latitudes and the 30°W and 52°W longitudes (Figure 1).

2.1. Conductivity-Temperature-Depth-Oxygen Data

Pressure, temperature, salinity, and dissolved oxygen measurements were acquired with a Neil Brown Mark III conductivity-temperature-depth-oxygen ($CTDO_2$) system, from the surface down to about 20 m above the bottom, with water samples for the sensor calibration and tracer measurements. The pressure and temperature sensors were

laboratory calibrated before and after each cruise. Water samples were used to calibrate the conductivity and oxygen sensors. For both CITHER cruises, pressure, temperature, salinity, and oxygen accuracies are about ±2 dbar, ±0.003°C, ±0.0025, and ±1.5 μmol kg^{-1}, respectively [*Le Groupe CITHER 1*, 1994a; *Le Groupe CITHER 2*, 1995]. For both ETAMBOT cruises the accuracies are about ±3 dbar, ±0.005°C, ±0.003, and ±1.5 μmol kg^{-1} [*L'Equipe ETAMBOT*, 1997a, b]. Unfortunately, for the ETAMBOT 2 cruise, neither salinity nor oxygen measurements are available for five stations located around 50°W, owing to sensors problems. Bottle samples are used at these locations. Furthermore, owing to a failure of the oxygen sensor, there are no $CTDO_2$ oxygen measurements along the whole 35°W section during this cruise.

2.2. Shipboard Acoustic Doppler Current Profiler Data

For each cruise, acoustic Doppler current profiler (ADCP) observations were collected continuously along the track lines. During the CITHER 1 cruise the ADCP profiler was a RDI 75 kHz. It provided absolute current measurements from 28 m to about 700 m depth, with a 16-m vertical bin resolution. During the CITHER 2 and both ETAMBOT cruises the ADCP profiler was a RDI 150 kHz, and absolute current measurements were obtained from 16 m to about 350-400 m depth over 8-m vertical bins. Owing to ADCP inboard installation problems, absolute current measurements are only available at the time of the $CTDO_2$ stations during the ETAMBOT 2 cruise. During each cruise, absolute referencing was provided by Global Positioning System (GPS); the shipboard system was calibrated as described by *Pollard and Read* [1989], using the Common Oceanographic Data Access System, version 3 (CODAS-3) of Hawaii University [*Bahr et al.*, 1990]. The original 5-min mean values have been averaged into "in stations" and "1/4°" profiles. The accuracy of these mean profiles is estimated through their standard deviation and is generally better than 5 cm s^{-1}; the mean standard deviation is about 3 cm s^{-1} [*Le Groupe CITHER 1*, 1994b; *Le Groupe CITHER 2*, 1996; *L'Equipe ETAMBOT*, 1997a, b].

3. Transports and water mass presentation

In the following sections we detail and analyze information about the main features of the circulation in the western equatorial Atlantic, i.e., the pathways, transports, and variability of (1) the main equatorial currents and (2) the South Atlantic origin water inflows and outflows and mesoscale features which affect the circulation.

While the SEC, NBC, NEC, and NECC commonly exhibit velocity core near the surface, the NBUC, EUC, SEUC, and NEUC velocity cores are found within and below the thermocline. Thus our description will be presented in two layers, based on these current distributions associated with density structures. For easier comparison with earlier studies, the upper layer is bounded by the sea surface and the 24.5 isopycnal surface [*Wilson et al.*, 1994; *Schott et al.*, 1995; *Bourlès et al.*, 1999] and the lower layer is bounded by the 24.5 and 26.75 isopycnal surfaces [*Bourlès et al.*, 1999]. West of 44°W, *Wilson et al.* [1994] and *Bourlès et al.* [1999]

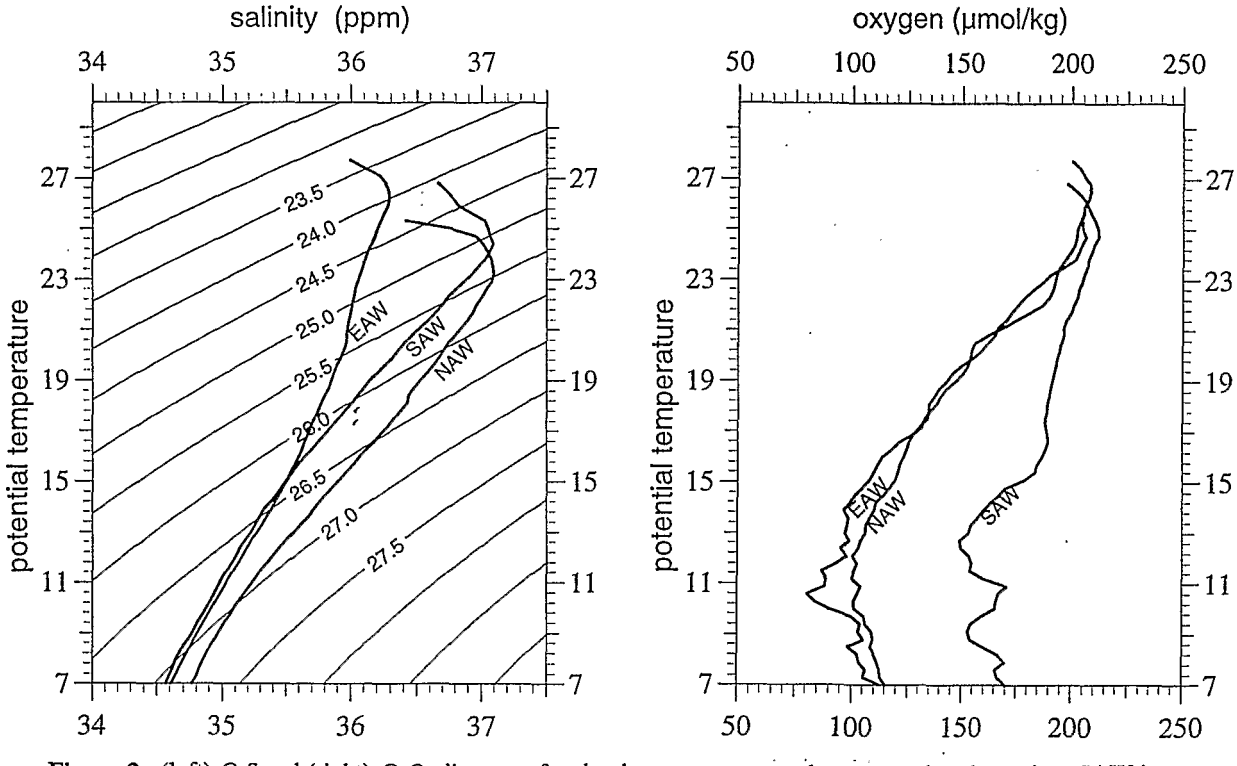

Figure 2. (left) Θ-S and (right) Θ-O_2 diagrams for the three water mass classes entering the region. SAW is a mean profile obtained west of 34°W along the 5°S section carried out in February 1993 during CITHER 1, representative of South Atlantic origin waters. EAW is a mean profile, obtained between 3°S and 1°S along 30°W in February 1994 during CITHER 2, representative of eastern tropical Atlantic origin waters. NAW is a mean profile obtained between 49°W and 47°W and between 11°N and 13°N in February 1994 during CITHER 2, representative of North Atlantic origin waters.

observe that the upper layer typically includes the NBC and NECC cores, whereas the lower layer includes the NEUC core. The 24.5 and 26.75 isopycnals are also used as boundaries for transport estimations. To compute the upper layer transports, the near-surface velocities were extrapolated to the surface using the first reliable ADCP measurement (slab layer approximation).

Water masses encountered in the western tropical Atlantic have been listed and described in many earlier studies [*Metcalf and Stalcup*, 1967; *Metcalf*, 1968; *Cochrane et al.*, 1979; *Emery and Dewar*, 1982; *Tsuchiya*, 1986; *Wilson et al.*, 1994; *Schott et al.*, 1995, 1998; *Bourlès et al.*, 1999]. From hydrographic measurements and tracers, *Arhan et al.* [1998] and M. Arhan and H. Mercier (A hydrographic section along the western boundary of the south and equatorial Atlantic, submitted to *Progress in Oceanography*, 1999) (hereinafter referred to as submitted manuscript, 1999) present a description of the water masses observed over the whole water column during the February 1993 and March 1994 cruises, respectively. We recall here the characteristics of the main water masses encountered in the upper layers of the region.

The first water mass is the North Atlantic Subtropical Underwater. Formed in the subtropics [*Worthington*, 1976], this water mass is characterized by high-salinity concentrations above the thermocline, in the $\sigma_0 = 24.5$-25.5 isopycnal range. The second water mass, the Southern Hemisphere counterpart of the Subtropical Underwater, is also characterized by high-salinity values above the thermocline [*Metcalf and Stalcup*, 1967]. These two water masses are advected equatorward within both subtropical gyres. A third water type commonly found in the western equatorial Atlantic has its source in the eastern tropical Atlantic and is carried into the study area by the SEC and the southern edge of the NEC [*Emery and Dewar*, 1982]. This water exhibits the lowest-salinity concentrations above the thermocline.

To differentiate the source regions of the waters over the whole upper column, three average temperature-salinity and temperature-oxygen curves have been computed, using $CTDO_2$ profiles carried out within currents advecting the three water masses described above into the region (Figures 1 and 2). The water entering the region from the northern tropical Atlantic (hereinafter referred to as NAW) exhibits the Subtropical Underwater salinity maximum of about 37.1 around the isopycnal $\sigma_0 = 25.5$ (Figure 2a). The water coming from the southern tropical Atlantic (hereinafter referred to as SAW) exhibits a salinity maximum of about the same value around the isopycnal $\sigma_0 = 25.0$. Note that the salinity maximum values for both NAW and SAW are attenuated during their course in the region; thus, for example, the SAW has lower-salinity maximum values than the NAW when it has reached the northwest of the study area [*Wilson et al.*, 1994; *Bourlès et al.*, 1999]. Below the thermocline the NAW is identified by the highest-salinity values (Figure 2a), while the SAW is clearly distinguishable by the highest-oxygen concentrations (Figure 2b). Finally, the water coming from the eastern tropical Atlantic (hereinafter referred to as EAW) is easily recognizable by the lowest salinity above and within the thermocline. Below, it exhibits similar salinity (respectively, oxygen) values to the SAW (respectively, NAW). The distinction between these waters becomes less obvious for the upper and well-mixed layer, above $\sigma_0 = 24.5$ (Figure 2). We note that currents measured along the 24.5 isopycnal surface

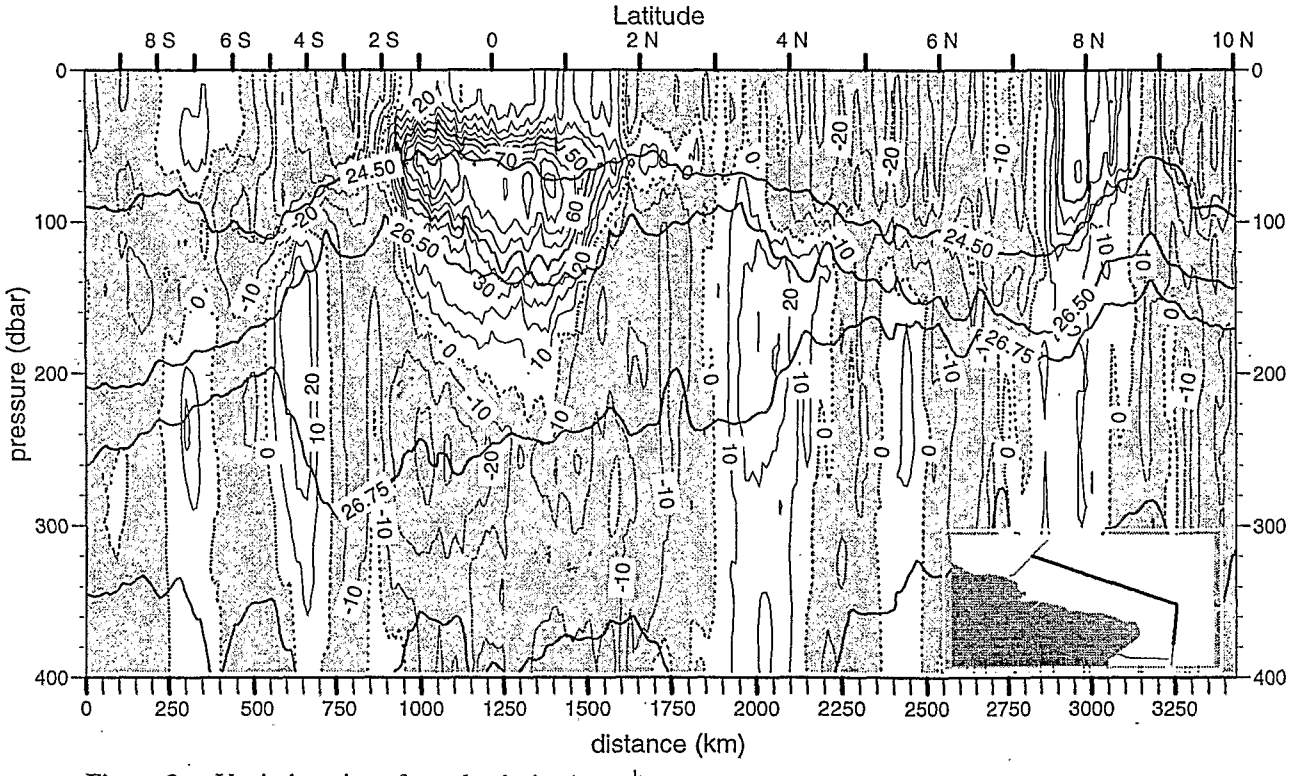

Figure 3a. Vertical section of zonal velocity (cm s^{-1}) component across the A17 World Ocean Circulation Experiment (WOCE) section in March 1994. Westward flow is shaded. Location of the sections is represented by the bold line in the map insets. Also shown are the 24.5, 26.50, 26.75, and 27.0 isopycnals.

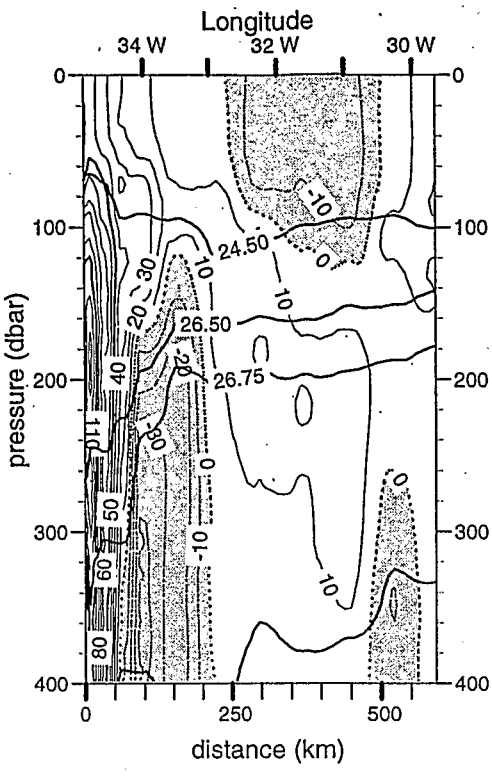

Figure 3b. Same as Figure 3.a. but for meridional velocity component at 5°S in February 1993, and with southward flow shaded.

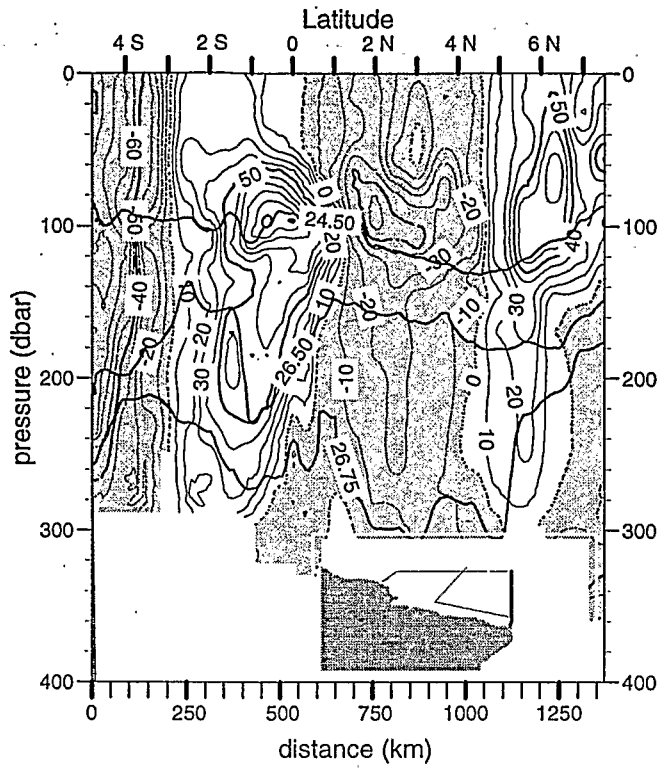

Figure 3d. Same as Figure 3.a. but for zonal velocity component at 35°W in September 1995.

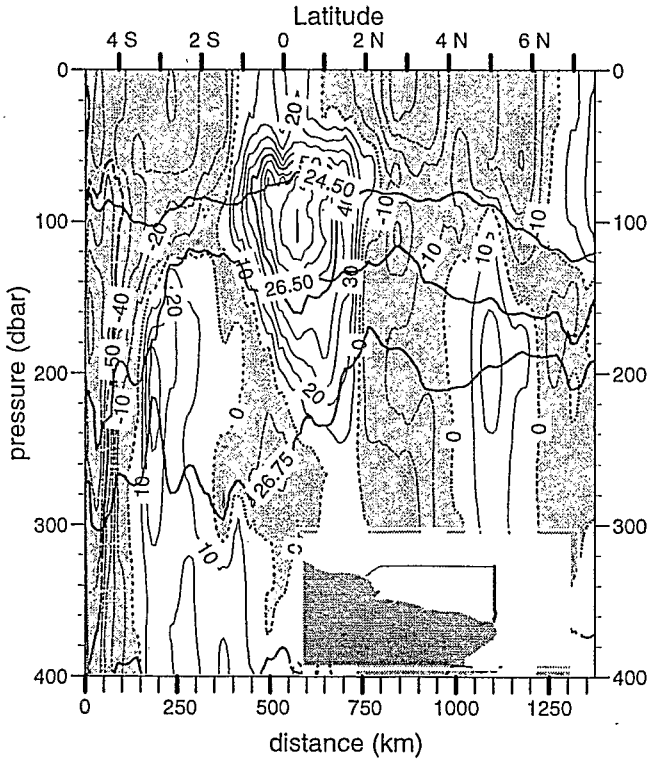

Figure 3c. Same as Figure 3.a. but for zonal velocity component at 35°W in February 1993.

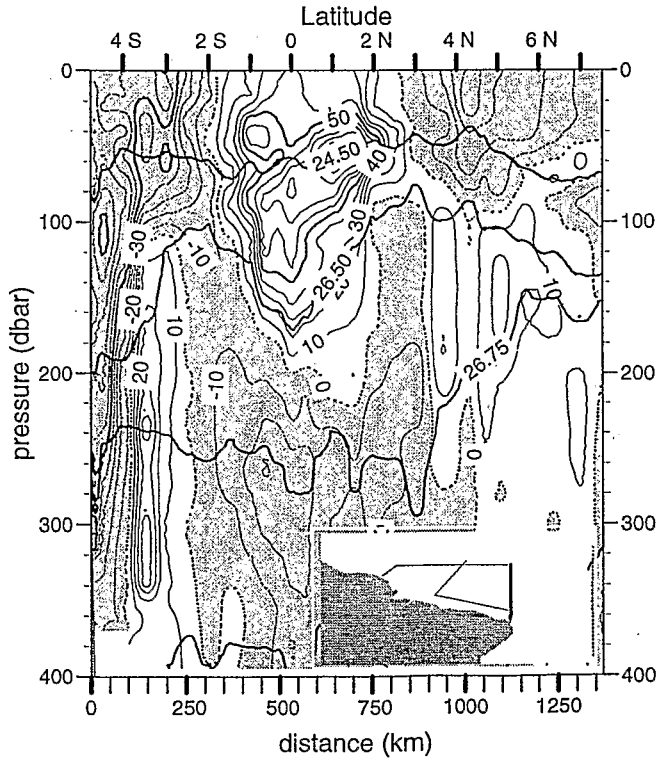

Figure 3e. Same as Figure 3.a. but for zonal velocity component at 35°W in April 1996.

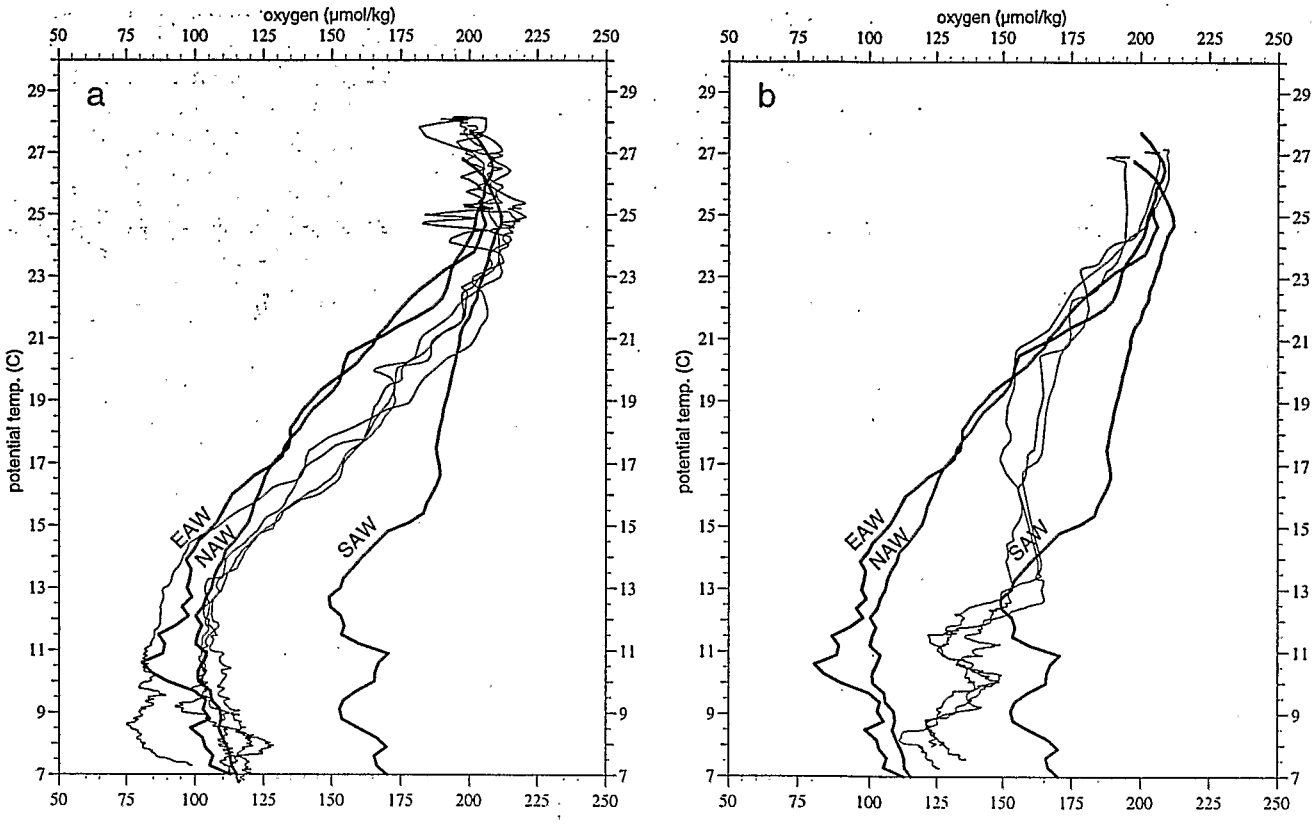

Figure 4. Θ-O_2 diagrams obtained in March 1994 (a) within the South Equatorial Countercurrent (SECC), between 6°S and 8°S, and (b) within the northern branch of the South Equatorial Current (SEC), between 2°N and 3°N.

are generally representative of the surface currents, as they extend up to the sea surface without any strong vertical shear or reversal (Figures 3a-3e). Therefore we will use the water mass properties on the 24.5 isopycnal surface to characterize the surface currents.

4. Analysis of equatorial currents

4.1. South Equatorial Countercurrent

Reid [1964] at 14°W and *Molinari* [1982] at 28°W describe an eastward flowing current, the South Equatorial Countercurrent (SECC), located between 6°S and 9°S. *Molinari* [1982] specifies that the SECC shows a subsurface velocity core with maximum velocities of 10 cm s^{-1} at 200-275 m. According to *Stramma and Schott* [1996], the SECC formation region has to be located near 30°W. While *Schott et al.* [1995] did not observe the SECC west of 30°W in March 1994, it is clearly observed during the nearly simultaneous CITHER 2 cruise at 30°W as an eastward flow extending from the surface down to at least 400 m depth, in the 6°S-8°S latitudinal belt (Figure 3a). In agreement with earlier observations, it exhibits a velocity core (20 cm s^{-1}) around 240 m depth. However, a second velocity core is present around 40 m depth, separated from the deeper velocity core by a westward flow (with significant westward velocity of about 9 cm s^{-1} near 7°S around 110 m depth). *Molinari* [1982, 1983] has noted that westward surface flow events may occur in boreal winter above the subsurface SECC velocity core. He suggests that while the SECC is geostrophically driven, strong southeast trade winds can induce westward reversals of the SECC during this period of the year. Such a previous westward reversal event, propagating down to 150 m depth, could explain the observed separation of the two SECC cores. While *Molinari* [1982] estimates the average transport of the SECC to 4 Sv at 25°W, the eastward SECC transport at 30°W is rather weak, as it is estimated to be about 0.5 Sv from the surface down to the 27.0 isopycnal.

From temperature and salinity distributions, *Molinari* [1982, 1983] indicates that the SECC is supplied, in the surface layers, with warm and salty subtropical waters by the southern branch of the SEC and that it exhibits lower salinities in the sublayers. As the SAW exhibits high oxygen concentrations over the whole water column under consideration, the low oxygen values measured within the SECC at temperatures lower than 19°C indicate that the SECC is also fed with EAW below the thermocline (Figure 4a).

4.2. North Brazil Undercurrent

From geostrophic calculations, *da Silveira et al.* [1994] have pointed out the existence of a velocity core centered at about 100-200 m depth, trapped along the Brazilian coast between 10°S and 5°S. This current, called NBUC by *Stramma et al.* [1995], carries equatorward the high-oxygen and high-salinity SAW within the thermocline layer [*Schott et al.*, 1995; *Arhan et al.*, 1998] and exhibits largest transports in boreal fall [*Stramma et al.*, 1995; *Schott et al.*, 1998]. The NBUC is observed along the westernmost part of the 4°30'S

Table 1. Transport Estimates (Sv) of the Main Currents in the Western Equatorial Atlantic

Current	Section	Date	Transport			
			σ_0<24.5 range	σ_0=24.5-26.75 range	σ_0=26.75 – 27 range	Total
NBUC	5°S	Feb. 1993	3.8	10.6		14.4
NBC	35°W	Feb. 1993	12.1	13.7		25.8
		Sept. 1995	11.1	12.7		23.8
		April 1996	8.6	15.4		24.0
	45°W	Sept. 1995	14.2	8.1		22.3
		April 1996	6.0	19.2		25.2
Retroflection[a]	44°W[b]	Sept. 1995	19.0	9.8		28.8
		April 1996	4.0	23.3		27.3
SEUC	35°W	Feb. 1993		3.1		
	30°W	March 1994		3.0		
	35°W	Sept. 1995		7.1[c]		
		April 1996		2.2		
EUC	35°W	Feb. 1993	4.9	17.6		22.5
	30°W	March 1994	7.2	14.4		21.6
	35°W	Sept. 1995	11.0	15.9[d]		26.9
	35°W	April 1996	11.4	16.9		28.3
NEUC	35°W	Feb. 1993		1.6	3.4	5.0
	38°W	March 1994		3.4	2.9	6.3
	35°W	Sept.1995		2.5[e]	1.3	3.8
		April 1996		3.6	3.3	6.9

Abbreviations are defined as follows: NBUC, North Brazil Undercurrent; NBC, North Brazil Current; SEUC, South Equatorial Undercurrent; EUC, Equatorial Undercurrent; NEUC, North Equatorial Undercurrent.
[a] Retroflection means the southeastward flow across the Ceara section, located offshore the NBC.
[b] Section was located at 44°W, between 3°N and 4°N.
[c] Isopycnal layer was 26.5-26.75.
[d] Isopycnal layer was 24.5-26.5.
[e] Isopycnal layer was 26.25-26.75.

section carried out in February 1993 (Figure 3b). It shows a subsurface core, roughly encompassed by the $\sigma_0 = 24.5$ and 26.75 isopycnals, with maximum velocities (up to 120 cm s^{-1}) from 150 to 300 m depth. While above $\sigma_0 = 24.5$ the northward transport is equal to 3.8 Sv, it amounts to 10.6 Sv in the $\sigma_0 = 24.5$-26.75 layer (Table 1). These values are close to the estimates of *Schott et al.* [1995, 1998] for the same year period, i.e., in March 1994 at 5°S (2.1 Sv above $\sigma_0 = 24.5$ and 11.1 Sv in the $\sigma_0 = 24.5$-26.8 isopycnal range) and March 1996 at 7°S (3.8 Sv and 10.9 Sv, respectively).

4.3. South Equatorial Undercurrent

From different sections carried out between 28°W and 25°W at different year periods, *Molinari* [1982] describes the SEUC as a subsurface-intensified eastward flow, located between 5°S and 3°S. Using expendable bathythermograph (XBT) data, *Reverdin et al.* [1991] observe that the SEUC flow is maximum in boreal fall and minimum in boreal spring around 30°W. The SEUC exhibits oxygen-enriched waters of southern origin [*Cochrane et al.*, 1979; *Tsuchiya*, 1986], and *Molinari and Johns* [1994] indicate that it is supplied out of a NBUC retroflection. Such a connection between those currents may explain why the seasonal cycles of the NBUC, at 10°S and 5°S, and the SEUC, around 30°W, are in phase. However, the SEUC is also fed by SEC oxygen-poor water [*Schott et al.*, 1995, 1998; *Arhan et al.*, 1998].

At 35°W, in February 1993 and April 1996, the SEUC is located between 4°S and 3°S; its velocity core (above 30 cm s^{-1}) is located between 200 and 300 m depth (Figures 3c and 3e). Its transport above the 26.75 isopycnal amounts to 3.1 Sv in February 1993 and 2.2 Sv in April 1996 (Table 1). At 30°W, in March 1994, the SEUC appears centered around 4°S, with a velocity core (>20 cm s^{-1}) above the 26.75 isopycnal (Figure 3a). While *Schott et al.* [1995] calculated a SEUC transport of 1.7 Sv in the 24.5-26.8 isopycnal range at 35°W during the same month, it amounts to 3.7 Sv in the same isopycnal range across 30°W (3.0 Sv above $\sigma_0 = 26.75$, Table 1). This eastward increase of the SEUC flow supports an additional supply by SEC waters along its eastward course.

A striking situation is observed in September 1995 (Figure 3d), when a unique eastward flow is visible between 3°S and the equator, extending from the surface down to at least 300 m depth. At depth this flow exhibits the signatures of the SEUC, with a marked deepening of the 26.75 isopycnal and a velocity core (>60 cm s^{-1}) around 200 m depth at 1°30'S. This feature indicates that the thermocline EUC and the subthermocline SEUC are vertically superimposed. To our knowledge it is the first time that the SEUC is observed so

north. During this cruise it is not possible to clearly distinguish the SEUC from the EUC. *Schott et al.* [1998] also observed a connection between the SEUC and the EUC in October 1990, i.e., in the same year period.

4.4. South Equatorial Current

South and north of the equator, the SEC carries westward low-salinity and low-oxygen EAW [*Emery and Dewar*, 1982; *Stramma*, 1991]. There is very little information about the seasonal cycle of these two SEC equatorial branches, which appear very weak in the western region [*Richardson and Walsh*, 1986; *Arnault*, 1987]. However, *Reverdin et al.*'s [1991] results suggest that, around 30°-35°W, the SEC northern (southern) branch is the strongest (weakest) in boreal summer-fall [see *Reverdin et al.*, 1991, Figure 9].

The SEC southern branch is clearly visible between 6°S and 1°30'S at 30°W, in March 1994 (Figure 3a). It exhibits a surface-intensified flow with velocities up to 60 cm s^{-1} at 3°S; its transport is equal to 11.6 Sv above $\sigma_0 = 24.5$.

The northern branch of the SEC extends farther north during the three boreal winter-spring cruises than in September 1995 (Figures 3a, 3c, 3d, and 3e). Its velocity rarely exceeds 30 cm s^{-1}. The westward transport of the northern branch of the SEC above $\sigma_0 = 24.5$ is equal to 8.5 Sv in February 1993, 12.3 Sv in September 1995, 4.5 Sv (as a minimum, due to incomplete coverage; Figure 3e) in April 1996 across 35°W, and 7.7 Sv between 39°W and 44°W in March 1994. The maximum value measured at 35°W during the boreal fall cruise supports the seasonal cycle suggested by the results of *Reverdin et al.* [1991]. The temperature-oxygen diagram of the profiles carried out between 2° and 3°N in March 1994 shows the presence of oxygen-enriched SAW within the SEC, below the thermocline (Figure 4b).

4.5. North Brazil Current

The southern branch of the SEC and the NBUC join and superimpose to form the NBC around 35°W off the Brazil coast, between 5°S and the equator [*Schott et al.*, 1995]. At 35°W, *Schott et al.* [1998] observe maximum NBC transports during boreal spring cruises, mainly due to subthermocline flow increases.

At 35°W, above $\sigma_0 = 24.5$, the westward flowing NBC exhibits varying width according to the cruise (Figures 3c-3e). While it extends until 1°S in February 1993, it is limited south of 3°S in September 1995, when it exhibits the highest zonal velocity (above 90 cm s^{-1} in the first 50 m depth). The NBC transport varies from a minimum of 8.6 Sv in April 1996 to a maximum of 12.1 Sv in February 1993 (Table 1). This variability is related to the depth of the 24.5 isopycnal surface, which is the shallowest in April 1996 (about 60 m depth), in agreement with the seasonal vertical displacement of the equatorial thermocline [*Merle and Arnault*, 1985; *Weisberg and Weingartner*, 1986]. In the $\sigma_0 = 24.5$-26.75 layer the NBC velocity core is found around 100 and 160 m depth, trapped against the continental slope. In this layer the NBC transport is maximum (15.4 Sv) in April 1996 (Table 1), in agreement with *Schott et al.*'s [1998] transport analysis and the seasonal cycle of the southern branch of the SEC suggested by *Reverdin et al.* [1991]. Note that the subthermocline NBC cycle is the opposite of the NBUC seasonal cycle observed by *Stramma et al.* [1995] at 10°S and 5°S. That difference may be explained by the retroflection of the NBUC in the SEUC. The mean NBC transport at 35°W between the sea surface and $\sigma_0 = 26.75$ is 24.5 Sv, of the same order of magnitude as the 27.8 Sv computed by *Schott et al.* [1998] above the isopycnal $\sigma_0 = 26.8$.

West of 35°W, the NBC continues northwestward along the Brazil coast. At 44°W its transport, computed between the sea surface and 300 m, is minimum in December-February (22.0±3.2 Sv) and maximum in June-August (27.8±4.4 Sv), with an annual mean of 23.8±4.6 Sv [*Schott et al.*, 1993]. A the same longitude, *Bourlès et al.* [1999] find, above the 26.75 isopycnal surface, a nearly similar mean NBC transport, amounting to 22.1±4.5 Sv, and the same seasonal cycle. Otherwise, *Schott et al.* [1993] measure strong NBC transport events (up to 30 Sv in March 1991), and *Bourlès et al.* [1999] observe large variations in the NBC transport at a 1-year interval for the same month. These variations are attributable to a strong short-term and interannual variability present in the region [*Johns et al.*, 1990; *Fratantoni et al.*, 1995; *Johns et al.*, 1998]. All these studies note the rapid increase of the NBC transport in June and that its maximum is always measured in late June or early July.

Vertical sections of the component of the velocity perpendicular to the Ceara section, between 45°W,0°N and 41°W,8°N, are shown in Figure 5. In the upper layer the NBC exhibits stronger velocity in September 1995 (110 cm s^{-1} at 50 m depth) than in April 1996. As observed at 35°W, the 24.5 isopycnal surface is deeper in September 1995 (120-140 m depth) than in April 1996 (60-80 m depth). Hence the NBC transport above $\sigma_0 = 24.5$ amounts to 14.2 Sv in September 1995 and 6.0 Sv in April 1996 (Table 1). In the subthermocline layer the NBC exhibits a subsurface velocity maximum, remnant of the NBUC core (Figure 5). Whereas this velocity core is located around 100 m depth with speed up to 130 cm s^{-1} in April 1996, it is found around 180 m depth with reduced speed (60 cm s^{-1}) in September 1995. Thus the NBC transport in the 24.5-26.75 isopycnal layer amounts to 8.1 Sv in September 1995 and 19.2 Sv in April 1996. The total NBC transport above the $\sigma_0 = 26.75$ surface across this section is equal to 22.3 Sv in September 1995 and 25.2 Sv in April 1996, i.e., slightly larger during the boreal spring cruise. This discrepancy with the seasonal cycle described by *Schott et al.* [1993] may be explained by the strong variability in the region. Also interesting is the consistency of the NBC flow from the sea surface down to the $\sigma_0 = 26.75$ isopycnal, between 35°W and 45°W (Table 1). However, this total transport masks the transport variations observed for each layer (Table 1). The transport variability is coherent with the $\sigma_0 = 24.5$ isopycnal depth variations, as it is deeper at 44°W than at 35°W in September, whereas it is at around the same depth in April. Such variations are in agreement with the wind stress seasonal cycle, related to the Intertropical Convergence Zone (ITCZ) latitudinal migration. In this region, when the ITCZ is at its northern location in boreal summer-fall, the southeasterly winds contribute to reinforce the surface flow and to deepen the thermocline. The *Johns et al.*'s [1998] analysis of the NBC seasonal cycle around 4°N,50°W in relation to the local and remote wind forcing supports this explanation. In the subthermocline layer ($\sigma_0 = 24.5$-26.75) the decrease of the NBC flow between 35°W and 44°W observed in September 1995 can be explained by a recirculation into the EUC; this point is more developed in section 4.7. However, we have no explanation for

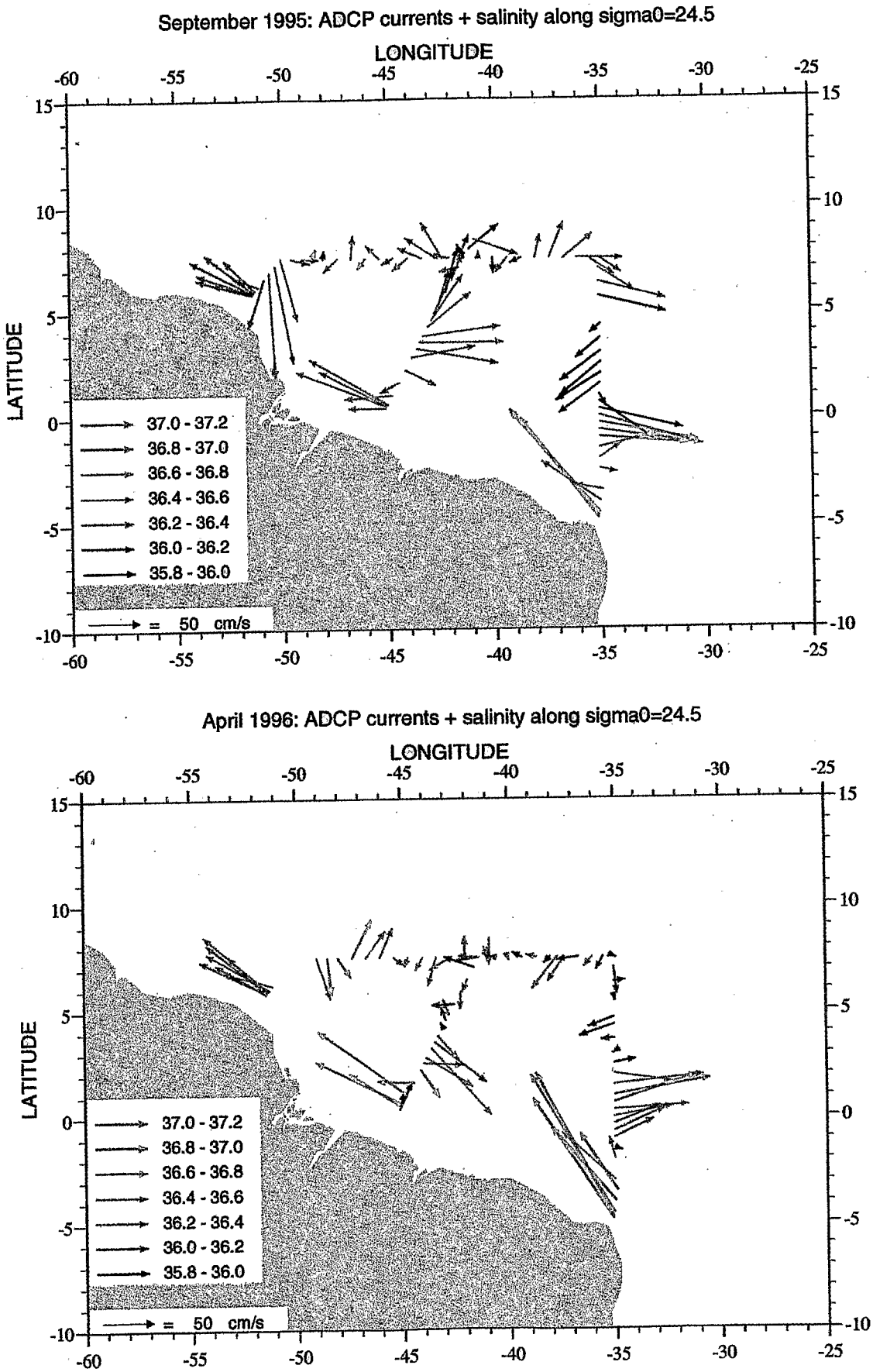

Plate 1. Current vectors and salinity concentration along the $\sigma_0 = 24.5$ surface in (top) September 1995 and (bottom) April 1996 (for details, see legend).

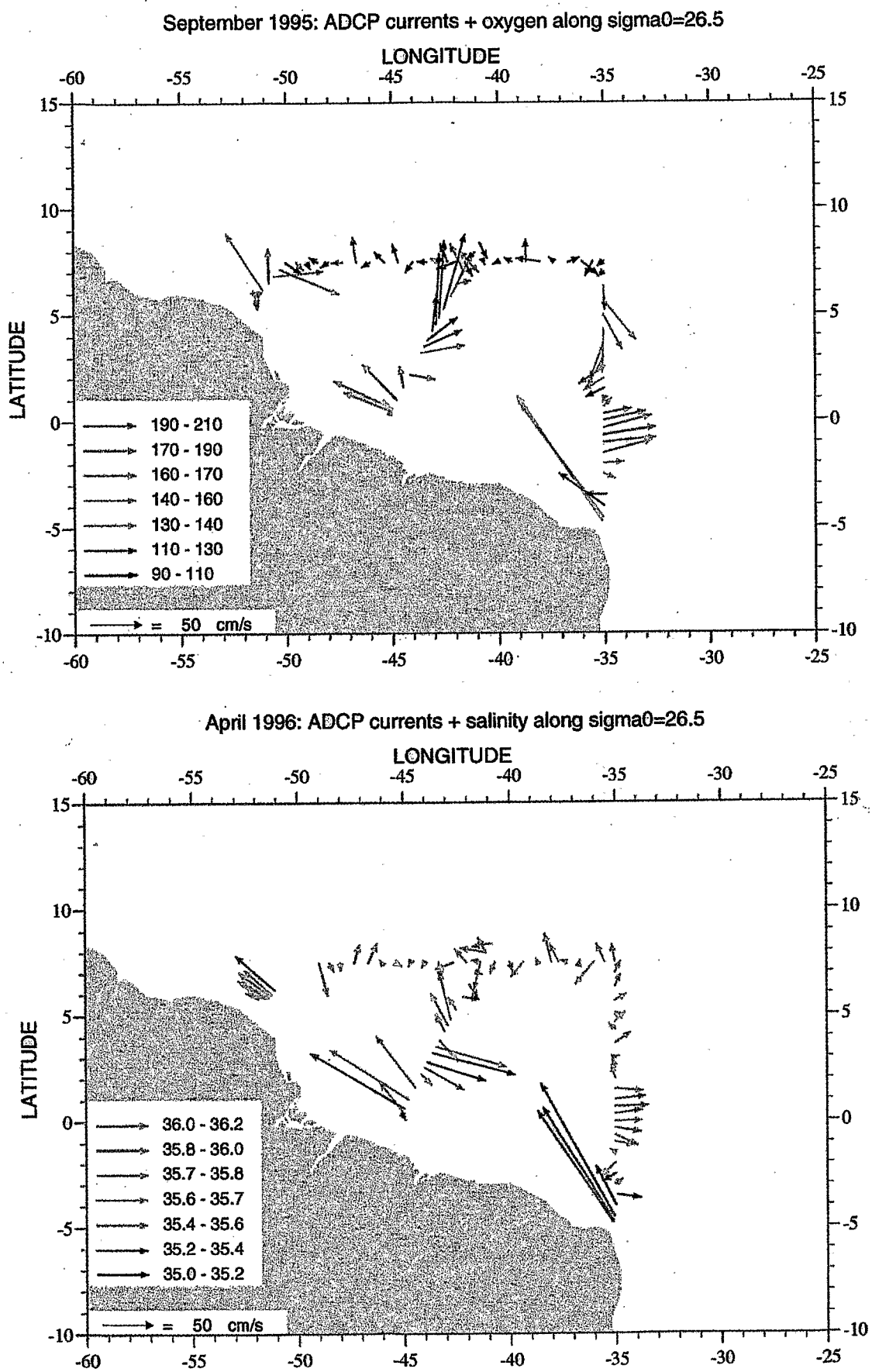

Plate 2. Current vectors along the $\sigma_0 = 26.5$ surface, along with (top) oxygen concentration in September 1995 and (bottom) salinity concentration in April 1996 (for details, see legend).

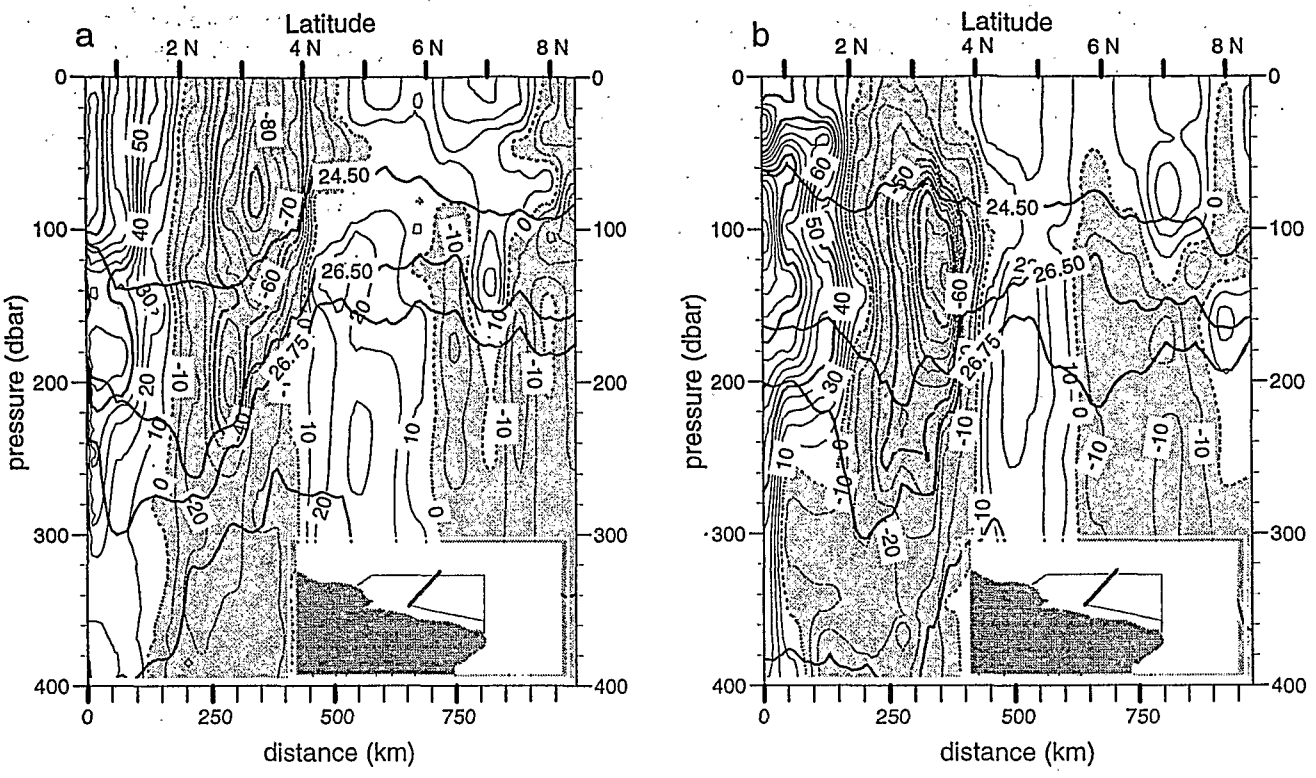

Figure 5. Vertical sections of the component of the velocity perpendicular to the Ceara section (cm s^{-1}), in (a) September 1995 and (b) April 1996. Southeastward flow is shaded.

the increase of 3.8 Sv (Table 1) observed in April 1996 between 35°W and 44°W, which is related to the intensification of the subthermocline velocity core.

4.6. Southeastward Flow at 45°W and Its Fate

After crossing the equator at 45°W, off the Amazon mouth, the NBC retroflection takes place. This retroflection is a source for the southeastward flow observed immediately north of the NBC across the Ceara section, around 3°N (Figure 5).

During both September 1995 and April 1996 cruises the southeastward flow exhibits a velocity core (up to 100 cm s^{-1}) at about the same depth (80 m) as the NBC core observed shoreward. A second velocity core (70 cm s^{-1}) is clearly visible in September 1995 at 200 m depth, at the same level as the NBC subsurface core (Figure 5a). The southeastward transport estimated between the sea surface and the 26.75 isopycnal surface is 28.8 Sv in September 1995 and 27.3 Sv in April 1996. These values exceed the northwestward NBC transports by about 2 to 5 Sv, depending on the cruise (Table 1). That means that even assuming a complete NBC retroflection, this flow is also supplied with NAW and/or EAW, advected into the region by the Northern Hemisphere SEC limb and by a NEC cyclonic recirculation, in agreement with earlier studies [*Molinari and Johns*, 1994; *Wilson et al.*, 1994; *Bourlès et al.*, 1999]. This point is illustrated by the horizontal velocity distribution on the 24.5 isopycnal surface, along with salinity concentrations, and on the 26.5 isopycnal surface, along with oxygen (in September 1995) and salinity (in April 1996) concentrations, presented in Plates 1 and 2. While in the upper layer, lower-salinity values are observed within the southeastward flow compared to those within the coastal NBC, in the subthermocline layer, NAW higher-salinity and lower-oxygen concentrations are observed at its northern edge, north of 3°N. In boreal summer-fall, *Bourlès et al.* [1999] estimate that this flow is fed by approximately two thirds of SAW in the upper layer and four fifths in the subthermocline layer. During the September 1995 cruise the southeastward transport above the 24.5 isopycnal amounts to 19 Sv, 5 Sv above the NBC transport, and in the subthermocline layer, it exceeds the NBC inflow by about 2 Sv. Assuming a total NBC retroflection at that time of the year, according to *Wilson et al.* [1994] and to *Bourlès et al.* [1999] and based on transport consideration only, these values suggest that the southeastward flow is composed of three fourths and four fifths of SAW in the upper and subthermocline layers, respectively, in good agreement with *Bourlès et al.*'s [1999] estimates.

The precise fate of this flow farther east is still a matter of debate. In the upper layer, *Wilson et al.* [1994] and *Bourlès et al.* [1999] identify the southeastward flow at 44°W as the NECC in boreal summer to winter, while *Schott et al.* [1995] show that it is connected to the shallow EUC in boreal spring. In the subthermocline layer, *Wilson et al.* [1994] and *Bourlès et al.* [1999] assimilate the southeastward flow to the NEUC in boreal summer to winter, while in their March 1994 cruise analysis, *Schott et al.* [1995] suggest that it connects directly with the EUC.

Cochrane et al. [1979] propose a basic scheme of the subthermocline circulation in the region for February-April and July-September composite data sets. They point out the presence, during both periods of the year, of an anticyclonic cell located around 4°N between 40°W and 35°W. Such a structure induces a large meandering behavior of the

retroflection flow, leading these authors to suggest that while a part of the southeastward flowing current observed at 45°W joins the EUC, the other part is deviated northward between 42°W and 40°W and then eastward to constitute the NEUC. Currents along $\sigma_0 = 26.5$ during both ETAMBOT cruises (Plate 2) agree with this circulation scheme [see *Cochrane et al.*, 1979, Figure 2]. During both cruises the southern edge of the flow observed around 3°N across the Ceara section exhibits a southeastward component, supporting a link with the EUC, while the northern edge of this current looks as if it is recirculating northwestward and eastward, in agreement with an eastward continuity within the NEUC. The currents on the $\sigma_0 = 26.5$ surface exhibit a similar circulation pattern on the $\sigma_0 = 24.5$ surface (Plate 1). This suggests that the anticyclonic feature observed by *Cochrane et al.* [1979] also extends upward within the upper water column; this point is supported by the vertical coherency of the currents observed along the Ceara section (Figure 5). In September 1995, part of the flow observed north of 2°N along this section also veers northward and eastward before joining the NECC visible along 7°30'N, east of 38°W (Plate 1, top). In April 1996 the northward and eastward recirculation is not observed, but the current and salinity distributions observed along the Ceara section and at 35°W agree with a direct linkage between the southeastward flow at 44°W and the upper EUC (Plate 1, bottom).

This circulation scheme is also in good agreement with the March 1994 observations presented by *Schott et al.* [1995]. While these authors suggest the presence of the EUC at 40°W between 2°N and 3°N, below the $\sigma_0 = 24.5$ surface they also observe a northward meandering flow north of 3°N at 35°W along the $\sigma_0 = 26.7$ surface [see *Schott et al.*, 1995, Figures 5c and 7]. Transport considerations led *Schott et al.* [1995] to attribute the eastward flow observed in March 1994 at 44°W in the subthermocline layer to be the source of the EUC, instead of the NEUC. As described in the following, currents measured in the subthermocline during our March 1994 cruise clearly show the NEUC around 38°W, between 3°N and 4°N (Figure 3a). Thus, while in September 1995 the southeastward flow observed across the Ceara section is interpreted as the source for the NECC and the upper EUC in the upper layer and for both the EUC and the NEUC in the subthermocline layer, in April 1996 it is interpreted as the source for both the EUC and the NEUC. Such a boreal spring circulation pattern is also supported by results obtained during a May-June 1991 *Meteor* cruise [*Schott et al.*, 1998].

4.7. Equatorial Undercurrent

In the western equatorial Atlantic the EUC velocity core is typically located above the thermocline [*Weisberg and Weingartner*, 1986; *Wacongne*, 1989]. The EUC core moves downward in boreal summer-fall and upward in boreal winter-spring, following the thermocline vertical migration [*Weisberg and Weingartner*, 1986]. However, evidence for a seasonal cycle of the EUC transport is still unclear. *Polonsky et al.* [1993] suggest that the EUC transport increases during the second half of the year; but, from a 2.7-year time series of currents at 0°,28°W, *Weisberg et al.* [1987] do not observe any replicating EUC annual cycle.

The eastward flowing EUC is characterized by a strong velocity core (up to 90 cm s^{-1}) around the 24.5 isopycnal depth (Figures 3a, 3c, 3d, and 3e). During every cruise an eastward near-surface flow is present above the EUC (at least up to the first ADCP measurements depth, either 16 or 28 m), with velocity up to 40 cm s^{-1} in April 1996. In boreal winter-spring, eastward equatorial near-surface currents have already been observed and are explained by the near-equatorial location of the ITCZ that leads to a relaxation of the wind forcing and an eastward pressure gradient [*Katz et al.*, 1981; *Weisberg and Weingartner*, 1986; *Richardson and Reverdin*, 1987; *Polonsky et al.*, 1993]. However, such a near-surface eastward flow is also observed between 2°S and the equator in September 1995 (Figure 3d) and was observed during two October cruises described by *Schott et al.* [1998]. Actually, from their 2.7-year time series of velocity carried out at 0°,28°W, *Weisberg et al.* [1987] mention a paucity of westward flow at 10 m depth. They indicate that the local wind stress does not seem to be the controlling element of the surface flow and point out the influence of the vertical advection of eastward momentum in the presence of large mean shear on the east component fluctuations. It is interesting to note that from numerical experiments carried out with the high-resolution WOCE Community Modeling Effort, *Schott and Böning* [1991], *Bryan et al.* [1995], and I. Wainer et al. (Dynamics of the Equatorial Undercurrent in a high-resolution ocean model, submitted to *Journal of Geophysical Research*, 1999) (hereinafter referred to as submitted manuscript, 1999) also observe such a surface eastward flow in boreal summer-fall, above the EUC core. All these authors explain the presence of this flow by the weakness of the vertical viscosity coefficient used in the model.

At 35°W the largest EUC transport, including the eastward near-surface flow, was measured in April 1996 (28.3 Sv) and the weakest occurred in February 1993 (22.5 Sv, Table 1). In March 1994 the EUC transport at 30°W amounts to 21.6 Sv, i.e., close to the 21.4 Sv calculated by *Schott et al.* [1995] at 35°W. Both our results and those of *Schott et al.* [1998] show that, if a seasonal cycle exists, it is strongly masked in boreal spring by wind trade relaxing, yielding to near-surface eastward jets and hence to strong eastward transport events. By only considering the subthermocline layer, beneath the $\sigma_0 = 24.5$ surface, the EUC flow does not indicate significant seasonal variations (Table 1).

We can note the presence of two velocity cores in March 1994, located at about 0°50'S and 0°50'N, centered on the 24.5 isopycnal (Figure 3a). Owing to the different longitudinal locations of these two cores (the southern one is at 30°W, and the northern one is around 33°W; see Figure 1) and as they have been measured at 2-day interval, this feature may be interpreted as a signature of the EUC meandering behavior. Large-scale meandering of the EUC has been documented at 28°W and 23°30'W by *Düing et al.* [1975], who observed an EUC core migration between the same latitudes.

In September 1995 and April 1996, high SAW salinity values (>36.6) present within the EUC core agree with a direct SAW supply through the NBC retroflection (Plate 1). However, fresh (<36.4) waters are also observed along its poleward boundaries. This indicates that EAW salinity-poor waters may also feed the EUC. That point, along with the presence of SAW within the northern SEC mentioned previously (Figure 4b), supports the existence of recirculations and water mass exchanges between the EUC and SEC, flowing in opposite directions.

4.8. North Equatorial Undercurrent

The existence of the NEUC was evidenced by *Cochrane et al.* [1979] west of 25°W, centered around 4°30'N, with maximum velocity of about 40 cm s^{-1}. These authors indicate that the NEUC transport significantly decreases from west of 40°W to the east and that the NEUC seems to break up in a number of filaments east of 28°W. Actually, as described above, *Cochrane et al.*'s [1979] description of the NEUC west of 40°W corresponds to the southeastward flow observed around 44°W that splits to feed different zonal currents, including the NEUC.

At 35°W, in February 1993 and April 1996, the NEUC is centered on 5°N with a 2° latitude width (Figures 3c and 3e). It is clearly observed between 3°N and 5°N around 38°W in March 1994 (Figure 3a). During these three cruises it exhibits a velocity core (>20 cm s^{-1}) close to the $\sigma_0 = 26.75$ isopycnal surface. In September 1995 the deepening of the isotachs and the 26.75 isopycnal, observed at 35°W around 5°-6°N, indicates the presence of the NEUC just beneath the NECC (Figure 3d).

The NEUC transport between the sea surface and the $\sigma_0 = 26.75$ surface varies from 1.6 Sv in February 1993 to 3.6 Sv in April 1996. In September 1995 the NEUC transport, estimated in the 26.25-26.75 layer, amounts to 2.5 Sv. In March 1994 we estimate 3.4 Sv around 38°W above $\sigma_0 = 26.75$, while *Schott et al.* [1995] find 1.8 Sv at 35°W above $\sigma_0 = 26.8$. *Cochrane et al.*'s [1979] observations do not suggest any significant NEUC seasonal cycle east of 40°W. Keeping in mind that our transport values may be underestimated owing to the incomplete vertical coverage, the NEUC transport exhibits higher values in boreal spring. Extending our estimates down to the $\sigma_0 = 27.0$ surface or down to the deepest available current measurement confirms that observation (Table 1).

Cochrane et al. [1979] indicate that the NEUC is supplied by the northern branch of the SEC as well as by the NEC. High-oxygen concentrations (in the 140-160 µmol kg^{-1} range) within the NEUC in September 1995 (Plate 2, top) show that this current is also supplied by SAW through the retroflection flow, in agreement with observations by *Schott et al.* [1998] and *Arhan et al.* [1998].

4.9. North Equatorial Countercurrent

The NECC exhibits a strong seasonal cycle. It is maximum in boreal summer-fall and remnant or even reversing westward in late boreal winter and spring, in relation to the seasonal migration of the ITCZ [*Richardson and Walsh*, 1986; *Arnault*, 1987; *Richardson and Reverdin*, 1987]. *Katz* [1993] specifies that the NECC reversing time length may be reduced to 1 month or extended to 4 months, owing to a large interannual variability, which has an amplitude comparable to the annual cycle. From inverted echo sounder (IES) measurements along 28°W, 38°W, and 44°W, *Garzoli* [1992] clearly shows that an eastward flow is present farther north in the 6°-9°N latitude range from February to April. From four boreal summer-fall cruises, *Bourlès et al.* [1999] estimate that the NECC is mainly fed by SAW through the NBC retroflection at this period of the year, with a SAW percentage of about 70%. In boreal winter, M. Arhan and H. Mercier [submitted manuscript, 1999] show that, in March 1994, the NECC was marked with NAW high-salinity values (>36.8), without any trace of SAW, whereas *Arhan et al.* [1998] observe SAW signatures in the NECC in February 1993.

In September 1995, at a time of the year when it is fully developed, the NECC is observed north of 5°N at 35°W and east of 42°W along 7°30'N (Figures 3d and 6b). The source of the NECC is the retroflection flow observed across the Ceara section (Plate 1, top). It then exhibits a meandering structure, as also observed from altimetric data by *Arnault et al.* [this issue]. Whereas *Schott et al.* [1995] do not observe any eastward NECC in March 1994, M. Arhan and H. Mercier [submitted manuscript, 1999] infer the presence of the NECC during this month from hydrological observations. An eastward current is actually present during the March 1994 cruise around 8°N,45°W (Figure 3a), i.e., north of *Schott et al.*'s [1995] survey. Its source is observed around 8°30'N,50°W along the section perpendicular to the coastline (Figure 6a), with a velocity core (up to 80 cm s^{-1}) at the same depth location (60 m) than farther east (Figure 3a). In April 1996 the NECC is not present at 35°W (Figure 3e). However, a flow with an eastward component is clearly present between 50°W and 45°W along the 7°30'N section (Plate 1, bottom, and Figure 6c). The high salinity (Plates 1 and 2, bottom) associated with low-oxygen (Figure 7) concentrations measured within this flow clearly indicate that it is fed only with NAW. These observations confirm that the NECC is still present in late boreal winter and remnant in spring at the western boundary, north and west of 7°N,40°W, and that it is

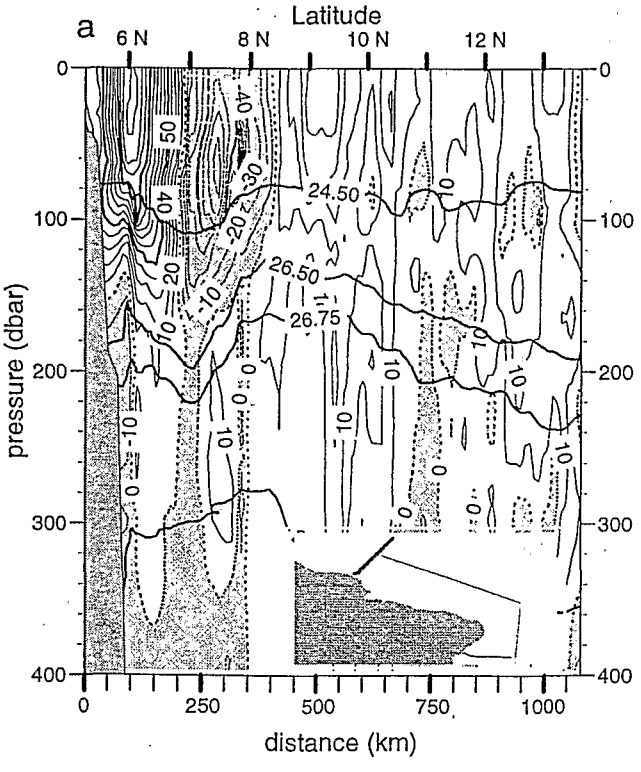

Figure 6. Vertical sections of (a) the component of the velocity (cm s^{-1}) perpendicular to the French Guiana section in March 1994, (b) the zonal velocity (cm s^{-1}) component along the 7°30'N section in September 1995, and (c) the zonal velocity (cm s^{-1}) component along the 7°30'N section in April 1996. The negative values, i.e., southeastward (Figure 6a) or westward (Figures 6b and 6c), are shaded.

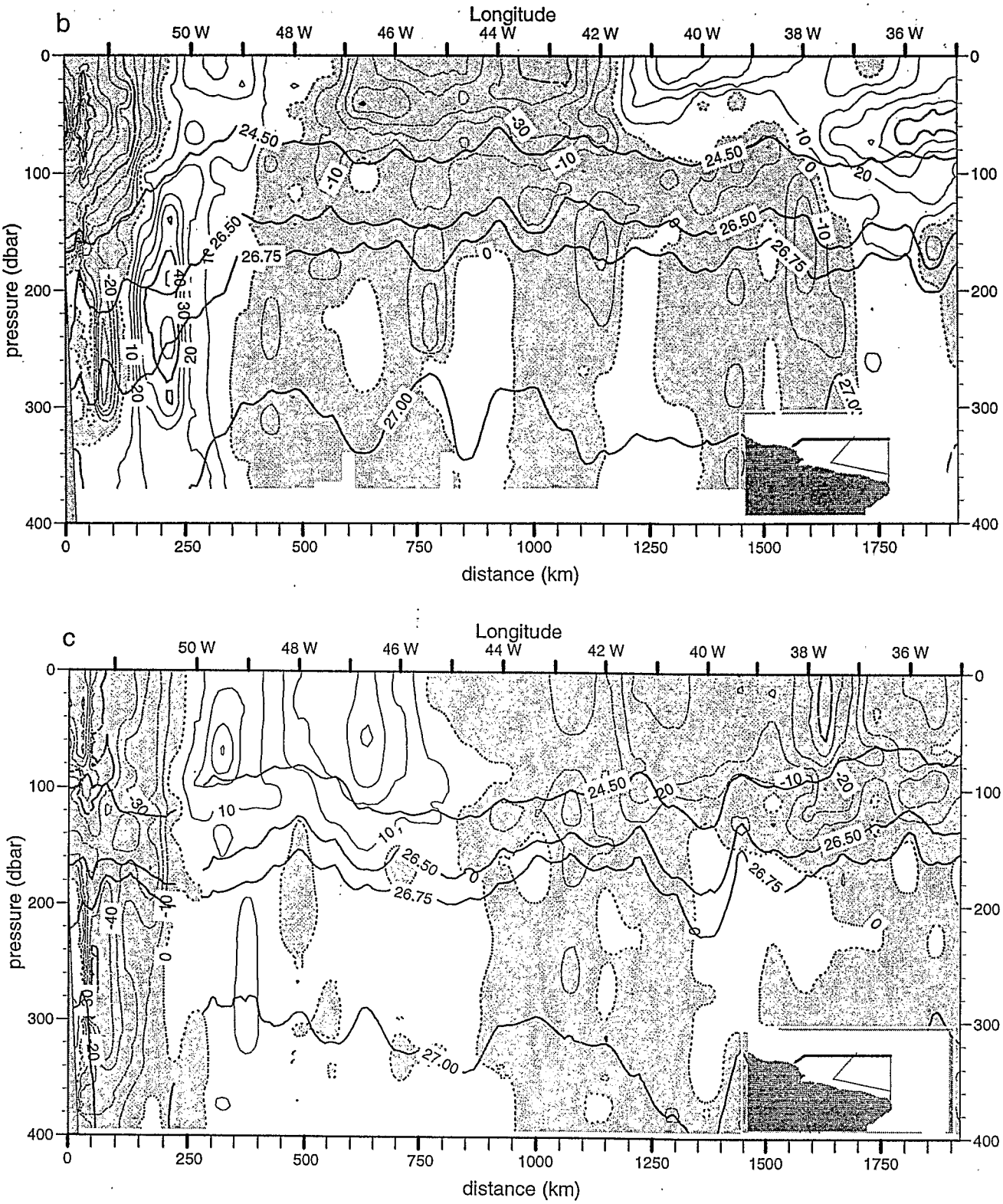

Figure 6. (Continued)

only fed with Northern Hemisphere waters in boreal spring, through the NEC cyclonic recirculation.

5. Analysis of the circulation off French Guiana

Some studies have shown that the NBC retroflection is total in boreal summer-fall and even in early winter [*Richardson and Reverdin*, 1987; *Richardson et al.*, 1994; *Wilson et al.*, 1994; *Bourlès et al.*, 1999]. *Schott et al.* [1995] and *Johns et al.* [1998] suggest that the NBC must continue northward along the western boundary in boreal spring, but they do not have any measurements north of 4°N to confirm this hypothesis. Thus the existence of a continuous SAW northwestward flow along the boundary is still questionable.

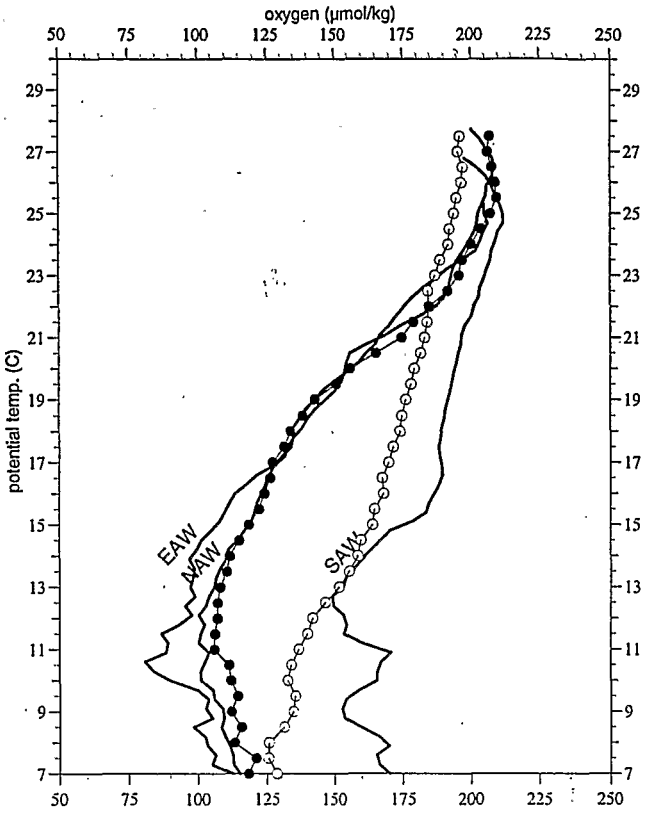

Figure 7. Θ-O_2 diagrams obtained off French Guiana in April 1996. Open circles represent the mean of the profiles located along the boundary, west of 51°W, and solid circles represent the mean of the profiles located offshore, in the 49°W-46°W longitude range.

Furthermore, the circulation in this region is strongly affected by mesoscale energetic variability, mainly owing to the presence of NBC retroflection eddies, that may mask the mean surface circulation [*Johns et al.*, 1990; *Richardson et al.*, 1994; *Fratantoni et al.*, 1995]. The section perpendicular to the French Guiana coastline, common to every cruise described herein, is located in a key region where the following can be observed: (1) the NBC retroflection loop [*Molinari and Johns*, 1994; *Wilson et al.*, 1994], (2) NBC retroflection eddies [*Johns et al.*, 1990; *Colin et al.*, 1994], and (3) the coastally trapped WBUC below the thermocline [*Colin and Bourlès*, 1994; *Wilson et al.*, 1994]. Furthermore, this section is north enough to observe an eventual direct SAW throughflow in boreal spring [*Johns et al.*, 1998]. Whereas the March 1994 and April 1996 cruises provide information about the SAW northward throughflow, the February 1993 and September 1995 cruises allow one to observe NBC retroflection eddies and describe their effect on currents and hydrological structures.

5.1. SAW Throughflow

In March 1994, M. Arhan and H. Mercier [submitted manuscript, 1999] infer, from $CTDO_2$ measurements, the northwestward continuation of the NBC off the French Guiana continental shelf. ADCP measurements confirm the presence of a strong coastal northwestward flow, with near-surface velocity as high as 120 cm s^{-1} at 6°N,52°W (Figure 6a). While this flow is characterized by SAW oxygen-enriched waters between the 22°C and 19°C isotherms (Figure 8, open circles), the southeastward flow observed just seaward between 7°N and 8°N does not contain any trace of SAW (Figure 8, solid circles). The SAW high-oxygen concentrations observed down to the 19°C isotherm indicate that the NBC continues its route toward the Caribbean within the subthermocline layer. The low-oxygen concentrations observed in the 14°C-18°C temperature range (Figure 8) are associated with a coastally trapped and weak southeastward flow located around and beneath the $\sigma_0 = 26.5$ isopycnal (Figure 6a). This is the signature of the WBUC. The net northwestward transport of SAW amounts to about 7.0 Sv above the $\sigma_0 = 26.75$ surface, including 5.0 Sv above $\sigma_0 = 24.5$.

In April 1996 a northwestward boundary flow is also observed off French Guiana, extending down to the subthermocline layer (Plates 1 and 2, bottom, and Figure 6c), and possessing high-oxygen SAW properties (Figure 7). Its transport is estimated to be 4.4 Sv above $\sigma_0 = 24.5$ and 2.5 Sv in the 24.5-26.75 isopycnal layer, yielding a total SAW northwestward throughflow of 6.9 Sv in April 1996, similar to the 7 Sv estimated in March 1994.

Seven additional $CTDO_2$ casts and ADCP profiles were carried out at the end of the ETAMBOT 2 cruise, in May 1996. Currents measured in the upper layer show a northeastward flow along the 7°30'N section east of 50°W, where a southeastward flow was observed 1 month earlier. Furthermore, the Θ-S diagrams obtained at a 1-month interval off French Guiana (Figure 9) indicate that while the onshore

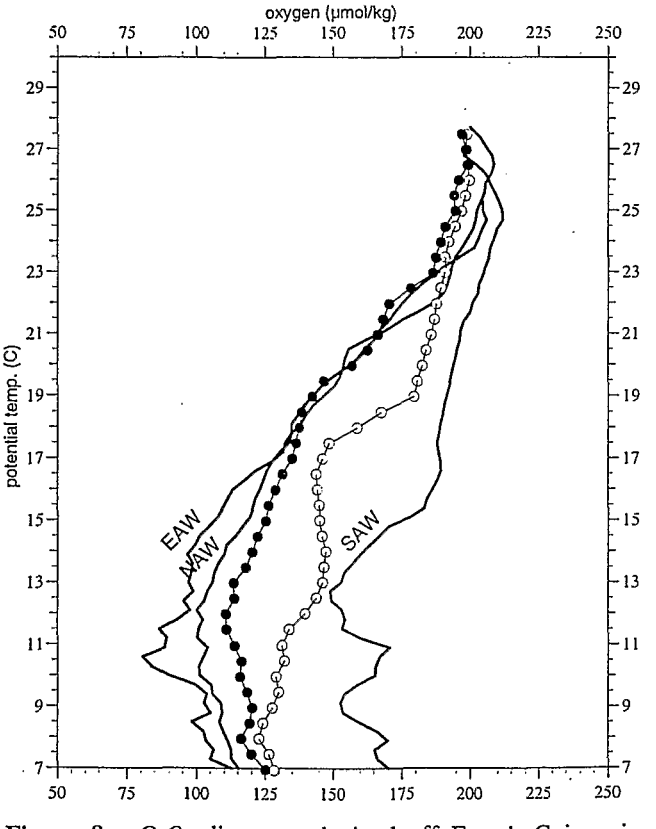

Figure 8. Θ-O_2 diagrams obtained off French Guiana in March 1994. Open circles represent the mean of the profiles located along the boundary, west of 51°W, and solid circles represent the mean of the profiles located just offshore, between 51°W and 50°W.

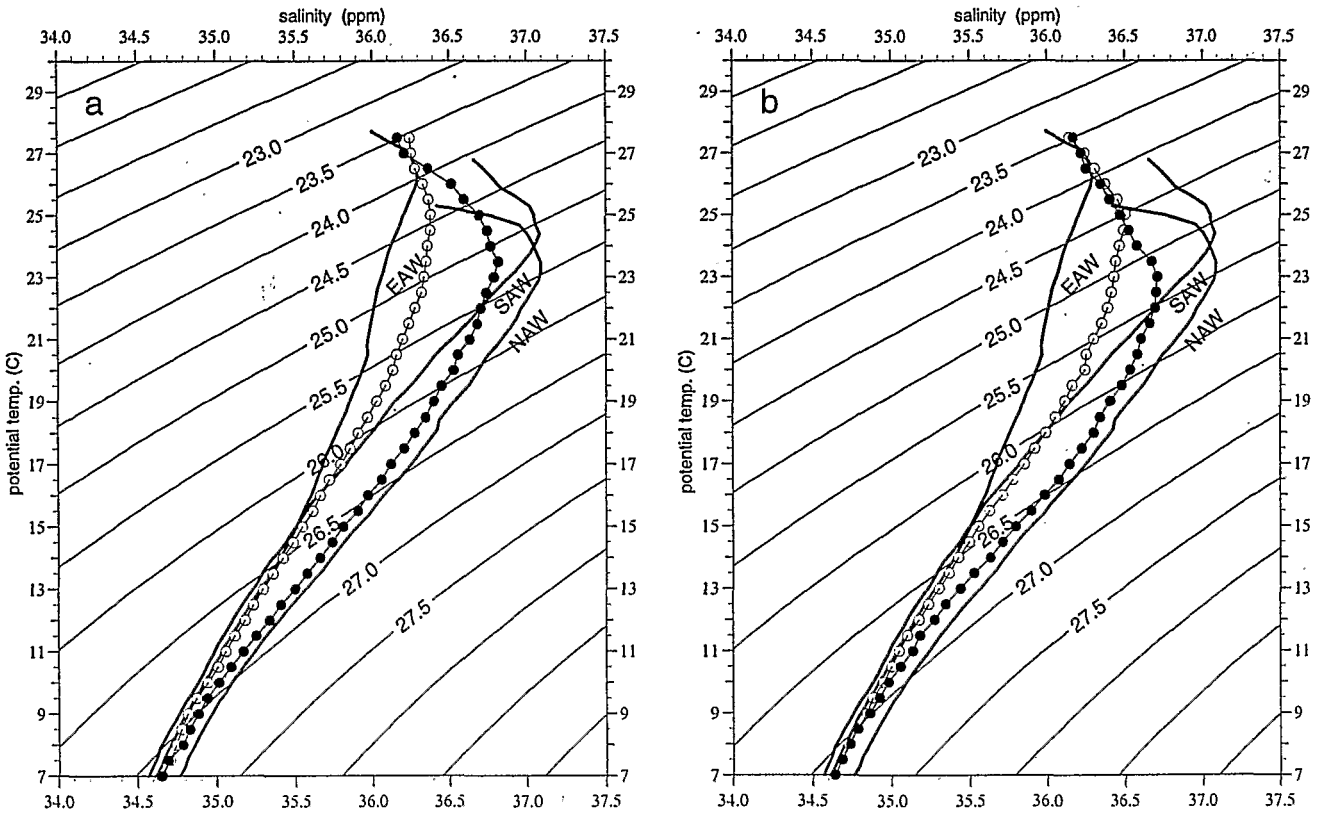

Figure 9. Θ-S diagrams obtained off French Guiana in (a) April 1996 and (b) May 1996. Open circles represent the mean of the profiles located along the boundary, west of 51°W, and solid circles represent the mean of the profiles located offshore, in the 51°W-46°W longitude range.

versus offshore Θ-S profiles are distinct at the beginning of the cruise, they are exactly superimposed at the end of the cruise, above the 24.5 isopycnal. This indicates that a partial NBC retroflection was present within the upper layer in May 1996. We estimate the transport of SAW toward the Caribbean Sea to be 1.9 Sv in May 1996 in the upper layer, i.e., 2.5 Sv smaller than 1 month earlier. Below the thermocline the SAW characteristics are found within a complex and unorganized current pattern, without any significant northward or southward transport.

5.2. NBC Retroflection Eddies

The role of the NBC retroflection eddies has been shown to be significant for the northward transport of warm water [*Johns et al.*, 1990; *Didden and Schott*, 1993; *Richardson et al.*, 1994]. These eddies are shed from the NBC retroflection zone, from boreal summer to winter, according to mechanisms that are not yet well understood [*Fratantoni et al.*, 1995]. *Johns et al.* [1990] and *Richardson et al.* [1994], from coastal zone color scanner (CZCS) satellite images and drifter trajectories, explain that an eddy formation entrains the NBC retroflection around 8°N,52°W, northwest of its usual location. When the eddy separates from the retroflection loop and translates northwestward, the retroflection returns to its initial position around 6°N,48°W. Observed NBC retroflection eddies may exhibit vertical penetration from 250 m down to 1000-1500 m depth [*Johns et al.*, 1990; *Richardson et al.*, 1994; *Fratantoni et al.*, 1995]. *Johns et al.* [1990] and *Colin et al.* [1994], from moored current meters located off French Guiana, and *Fratantoni et al.* [1995], from numerical experiments, suggest that NBC retroflection eddies propagate from the subthermocline layers. *Bourlès et al.* [1999, Figure 9] present a vertical section of the velocity across a NBC retroflection eddy observed in January 1991 that bears evidence that the vertical axis of the eddy is bent with a northwestward slope according to depth.

In February 1993 an anticyclonic structure is observed off French Guiana, with velocity up to 100 cm s^{-1}, associated with a deepening of the isopycnals (Figure 10). The superimposition, above the 25.5 isopycnal, of the Θ-S diagrams obtained at the western and eastern edges of this structure indicates that the water circulates within a closed loop in the upper layer (Figure 11). Dominant SAW characteristics observed within this structure down to about the $\sigma_0 = 26.0$ isopycnal (Figure 11) indicate that this structure is an anticyclonic eddy issued from the NBC retroflection. The presence of a NBC retroflection eddy in this area and at this time is also strongly suggested by the TOPEX/POSEIDON altimeter measurements (S. Arnault, personal communication, 1997). Below this eddy and the 26.5 isopycnal the coastally trapped southeastward flow (Figure 10) along with the presence of NAW characteristics (Figure 11) are the signature of the WBUC. ADCP measurements, acquired at 150 m depth during the transit between the 35°W survey and the Cayenne call, clearly show the presence of the WBUC along the boundary (Figure 12). It extends 100 km

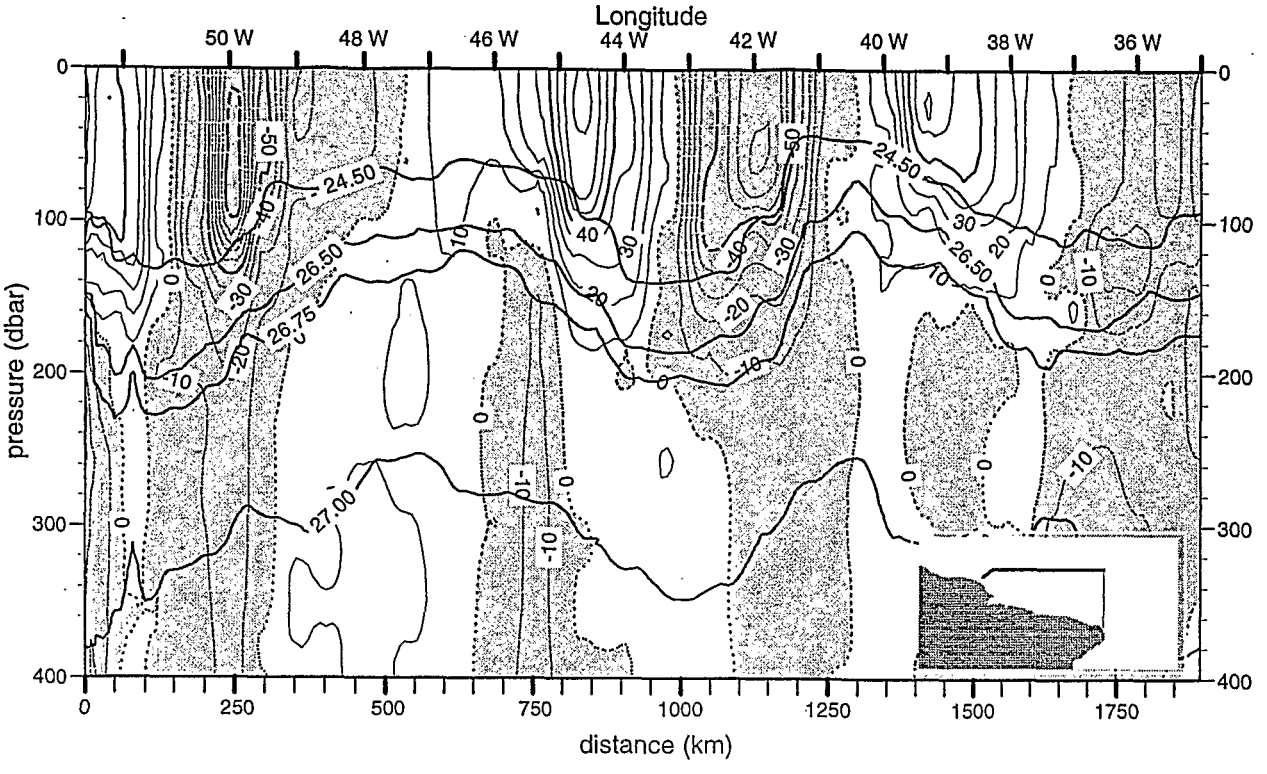

Figure 10. Vertical sections of the component of the velocity (cm s^{-1}) perpendicular to the 7°30'N section in February 1993. The negative values, i.e., southeastward (at the westernmost part of the section) or southward, are shaded.

offshore between the continental slope and an anticyclonic structure associated with the subthermocline NBC retroflection.

In September 1995 an anticyclonic, eddy-like structure is observed off French Guiana in the upper layer (Plate 1, top). Such an eddy is also clearly inferred from TOPEX/POSEIDON altimeter measurements [*Arnault et al.*, this issue]. In the subthermocline layer, oxygen-enriched SAW is observed around 51°W,6°N in an anticyclonic structure associated with the NBC retroflection (Plate 2, top). ADCP measurements carried out at 50 m depth at the end of the cruise, in October 1995, indicate the presence of a large, anticyclonic structure, at the same location where we observed an anticyclonic eddy structure 1 month earlier (Figure 13).

Thus, during both February 1993 and September 1995 cruises, while the southern edge of a NBC retroflection eddy is observed in the upper layer, the NBC retroflection is present in the subthermocline layer. These observations agree with and confirm a northwestward translation of the NBC retroflection eddies first occurring in the subthermocline layer.

In February 1993 the WBUC is weak and with a smaller offshore extent at 6°N, where a NBC eddy is present (Figure 10), than farther south (Figure 12). This is in agreement with the analyses of *Wilson et al.* [1994] and *Bourlès et al.* [1999], who indicate that the coastal WBUC is deviated offshore and around the NBC retroflection eddies, then coastally trapped south of the eddies before being entrained eastward by the NBC retroflection, contributing to the eastward equatorial countercurrent's water supply.

6. Conclusions

In this study, $CTDO_2$ and ADCP measurements, obtained during four cruises carried out in February 1993, March 1994, September 1995, and April 1996, are used to analyze the circulation in the upper layer of the western tropical Atlantic Ocean. These observations allow clarification of some characteristics of the currents and patterns of the warm water northward pathway in this region. Many aspects of each circulation element analyzed in this paper have been described in earlier studies. We now point out and discuss the features of the circulation that our measurements allow us to understand better.

6.1. Pathways for SAW Supply of Eastward Equatorial Currents

After entering the western equatorial Atlantic, some of the SAW advected within the NBUC and the NBC retroflects and supplies the eastward currents (SEUC, EUC, NEUC, and NECC). The NBUC and the SEUC, which exhibit the same seasonal cycles, are directly linked through a partial NBUC eastward recirculation. By contrast, the eastward pathway of the SAW is more complex farther north and occurs mainly through the NBC retroflection, which supplies dominantly the southeastward current observed around 3°N,44°W. The data sets of the four cruises presented here indicate that this southeastward current feeds, in the upper layer, the NECC and the upper EUC from boreal summer to early winter, while it is a source for the upper EUC in boreal spring. In the

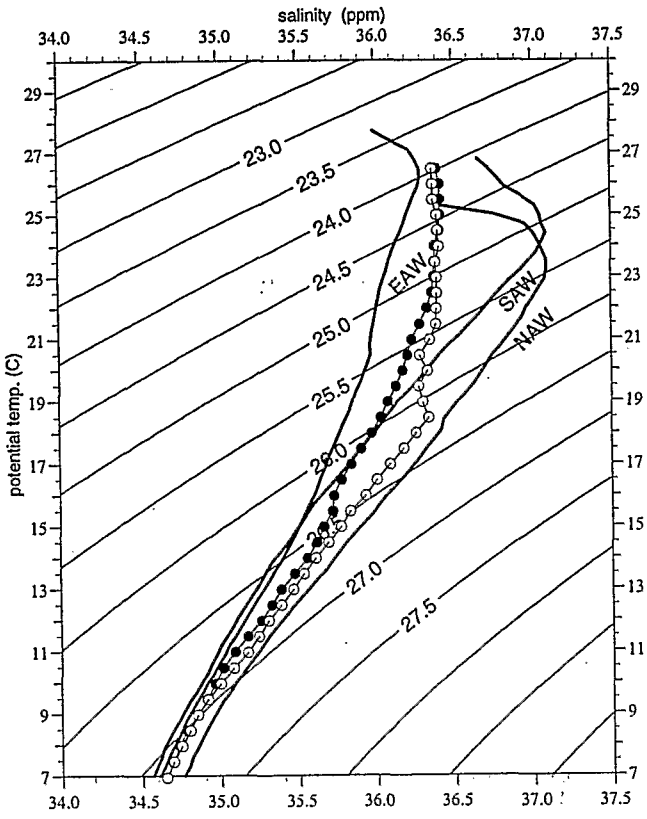

Figure 11. Θ-S diagrams obtained off French Guiana in February 1993. Solid circles represent the mean of the profiles located at the western edge of the anticyclonic eddy. Open circles represent the mean of the profiles located at the eastern edge of the anticyclonic eddy.

thermocline layer, part of this flow continues southeastward and joins the EUC, while the remainder meanders northeastward then eastward to form the NEUC; hence it is a source for both the EUC and the NEUC. In addition to *Cochrane et al.*'s [1979] circulation scheme discussed in section 4.6, this circulation pattern is also in good agreement with numerical results of the WOCE Community Modeling Effort [*Schott and Böning*, 1991] and with the simple ocean box model of *Gu and Philander* [1997], who suggest a linkage between the subtropical and tropical Atlantic through shallow overturning cells. This linkage requires splitting of the retroflection flow, with part of this current joining the EUC. This circulation pattern also explains the large overestimates in previous studies of the NEUC transport west of 40°W, the retroflection flow being assimilated to the NEUC, instead of its source.

6.2. Direct Northwestward SAW Throughflow

In boreal summer to winter, many studies indicate that the NBC retroflection seems to be total [*Richardson et al.*, 1994; *Wilson et al.*, 1994; *Bourlès et al.*, 1999], yielding to the absence of any direct SAW throughflow toward the Caribbean. On the contrary, in boreal spring, *Schott et al.* [1995] and *Johns et al.* [1998], from measurements carried out south of 4°N, suggest that the NBC must continue northward along the western boundary. The circulation observed in March 1994 and April-May 1996 off French

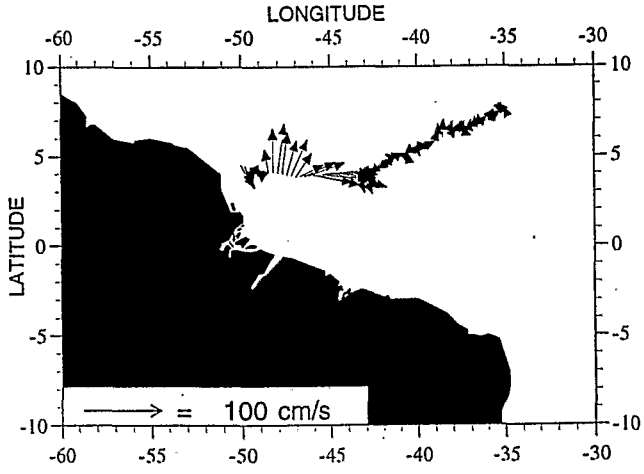

Figure 12. Current vectors at 150 m depth in February 1993, measured along the transit route from 7°30'N,35°W to the Cayenne call during the CITHER 1 cruise.

Guiana, i.e., north enough to verify this possibility, confirms this direct NBC northwestward continuity. However, contrary to these authors, who do not provide evidence of any significant continuous flow in the subthermocline layer, our results show that a weak part of the direct SAW throughflow may also occur in this layer, at least in March and April. *Schott et al.* [1998] estimate, from cruises made in March 1994 and March 1996, that 12 Sv of SAW may continue northwestward along the boundary, whereas we estimate a transport of about 7 Sv in March 1994 and April 1996. We explain this difference by a partial NBC retroflection that supplies the upper EUC and the NEUC, as shown in section 4.8. In March 1996, *Schott et al.* [1998] estimate the same transport of 12 Sv around 5°N and 10°N; but the data coverage during this cruise is relatively poor, and these authors clearly mention that they could not, from salinity only, distinguish between southern waters and those coming from out of the northern subtropics. Actually, their measurements were carried out where the boundary northwestward flow, here called the Guiana Current, is also fed with NEC water, as shown by *Metcalf* [1968].

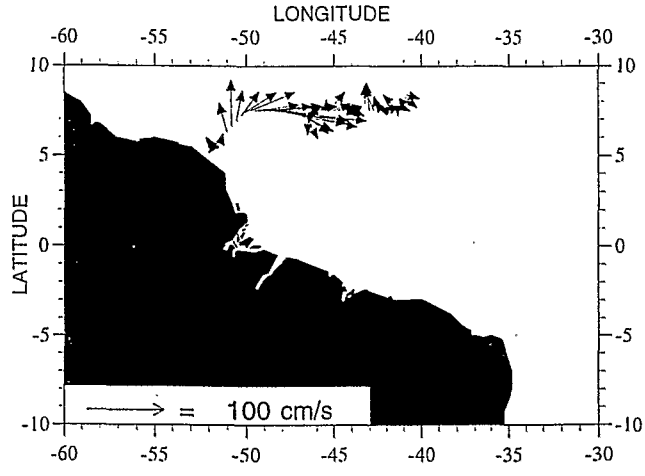

Figure 13. Current vectors at 50 m depth in October 1995, at the end of the ETAMBOT 1 cruise.

6.3. NAW Pathway

Mayer and Weisberg [1993], using 40 years of Comprehensive Ocean-Atmosphere Data Set (COADS) information to describe the Sverdrup wind-driven circulation, show that while the clockwise equatorial gyre is closed by the NBC retroflection along the western boundary, a cyclonic flow, i.e., a southeastward boundary current, is required farther north to complete the return flow of the North Atlantic cyclonic tropical gyre. In the near-surface layer, *Bourlès et al.* [1999] observe that such a flow is ensured by a NEC cyclonic recirculation in boreal summer and winter, feeding the NECC with NAW. The data sets presented here confirm this NEC recirculation, even during the two boreal spring cruises, and indicate its yearlong permanency. From boreal summer to winter this NEC recirculation joins with the NBC retroflection flow and constitutes a NAW supply for the NECC and the NEUC. In boreal spring, remnants of the NECC are observed along the boundary, which are only fed with NAW. In the subthermocline layer the southeastward boundary flow required in the analysis of *Mayer and Weisberg* [1993] is ensured by the WBUC, advecting NAW toward the equator. While *Bourlès et al.* [1999] did not witness this flow during two January cruises, it is clearly observed in February 1993. The WBUC is not observed along the continental shelf south of the NBC retroflection zone and hence becomes totally entrained in the southeastward flow observed across the Ceara section. While this flow feeds both the NEUC and the EUC, we could expect that the WBUC might contribute to the EUC supply, as suggested by *Schott and Böning* [1991] from numerical experiments. However, no NAW properties have been evidenced within the EUC.

6.4. Short Scales Processes

The data of the four cruises exhibit an eastward near-surface jet above the EUC, even in boreal fall. It is noticeable that such a feature is also present throughout the year in numerical simulations of the WOCE Community Modeling Effort [*Schott and Böning*, 1991; *Bryan et al.*, 1995; I. Wainer et al., submitted manuscript, 1999]. It is not yet clear if that eastward flow is due to the trade winds relaxing events, to the permanency of the NBC retroflection, even partial in boreal spring, or to vertical advection of eastward momentum, as suggested by *Weisberg et al.* [1987]. It has been shown that this flow would be responsible for a SAW eastward transport that is far from negligible.

The water mass analysis indicates that recirculations and water exchanges exist between the main equatorial currents, such as between the SEC and the EUC. In the Pacific Ocean, *Kennan* [1997] explains that the vortex structures observed between the SEC and the NECC, and also between the SEC and the EUC, are primarily due to barotropic instability caused by the zonal current shear, instead of equatorial waves. He shows that such features may generate recirculation cells between opposite equatorial currents and countercurrents, which are responsible for water mixing and exchanges.

Finally, a striking situation is observed in September 1995, when the EUC and the SEUC as well as the NECC and the NEUC appear superimposed. The same feature was observed by *Schott et al.* [1998] between the SEUC and the EUC in October 1990 and by *Bourlès et al.* [1999] between the NECC and the NEUC in September 1990 and September 1991. Whether such a feature is linked to the NBC retroflection eddy formation events, which occur mainly in boreal summer-fall, and/or to short-scale wave-like instabilities propagating from the basin interior, must also be investigated.

Acknowledgments. These cruises have been supported by ORSTOM (ETAMBOT and CITHER 1) and IFREMER (CITHER 1 and CITHER 2) as part of the Programme National d'Etude de la Dynamique du Climat of Institut National des Sciences de l'Univers (INSU), and its WOCE/France subprogramme. CITHER 1 and both ETAMBOT cruises have been realized principally thanks to Claude Oudot to whom we are particularly grateful. We specially thank all our colleagues from IRD (formerly ORSTOM) and Laboratoire de Physique des Océans/Brest (LPO), Jean-Michel Boré, Gérard Eldin, François Baurand, André Billant, Catherine Lagadec, and Pierre Brannelec, who contributed to the preparation, realization, and calibration of the measurements. We acknowledge Chantal Andrié, Michel Arhan, Sabine Arnault, Sophie Wacongne, Herlé Mercier, Fritz Schott, Bill Johns, and Ilana Wainer for helpful comments and discussions on this work and also for having given us early versions of their unpublished works.

References

Arhan, M., H. Mercier, B. Bourlès, and Y. Gouriou, Hydrographic sections across the Atlantic at 7°30'N and 4°30'S, *Deep Sea Res., Part I, 45*, 829-872, 1998.

Arnault, S., Tropical Atlantic geostrophic currents and ship drifts, *J. Geophys. Res., 92*, 5076-5088, 1987.

Arnault, S., B. Bourlès, Y. Gouriou, and R. Chuchla, Intercomparison of the upper layer circulation of the western Equatorial Atlantic Ocean: In situ and satellite data, *J. Geophys. Res.*, this issue.

Bahr, F., E. Firing, and S. Jiang, Acoustic Doppler current profiling in the western Pacific during the US-PRC TOGA Cruises 5 and 6, *Data Report No. 007, JIMAR Contract 90-0228*, 162 pp., Univ. of Hawaii at Manoa, Honolulu, 1990.

Bourlès, B., R. L. Molinari, E. Johns, W. D. Wilson, and K. Leaman, Upper layer currents in the western tropical North Atlantic (1989-1991), *J. Geophys. Res., 104*, 1361-1376, 1999.

Bryan, F. O., I. Wainer, and W. Holland, The sensitivity of the tropical circulation in an eddy resolving North Atlantic model to the specification of wind stress climatology, *J. Geophys. Res., 100*, 24,729-24,744, 1995.

Cochrane, J. D., F. J. Kelly Jr., and C. R. Olling, Subthermocline countercurrents in the western equatorial Atlantic Ocean, *J. Phys. Oceanogr., 9*, 724-738, 1979.

Colin, C., and B. Bourlès, Western boundary currents and transports off French Guiana as inferred from Pegasus observations, *Oceanol. Acta, 17*, 143-157, 1994.

Colin, C., B. Bourlès, R. Chuchla, and F. Dangu, Western boundary current variability off French Guiana as observed from moored current measurements, *Oceanol. Acta, 17*, 345-354, 1994.

da Silveira, I. C. A., L. B. de Miranda, and W. S. Brown, On the origins of the North Brazil Current, *J. Geophys. Res., 99*, 22,501-22,512, 1994.

Didden, N., and F. A. Schott, Eddies in the North Brazil Current retroflection region observed by Geosat altimetry, *J. Geophys. Res., 98*, 20,121-20,131, 1993.

Düing, W., et al., Meanders and long waves in the equatorial Atlantic, *Nature, 257*, 280-284, 1975.

Emery, W. J., and J. S. Dewar, Mean temperature-salinity, salinity-depth and temperature-depth curves for the North Atlantic and the North Pacific, *Prog. Oceanogr., 11*, 219-305, 1982.

Fine, R. A., and R. L. Molinari, A continuous deep western boundary current between Abaco (26.5°N) and Barbados (13°N), *Deep Sea Res., Part A, 35*, 1441-1450, 1988.

Flagg, C. N., R. L. Gordon, and S. McDowell, Hydrographic and current observations on the continental slope and shelf of the western equatorial Atlantic, *J. Phys. Oceanogr., 16*, 1412-1429, 1986.

Fratantoni, D. M., W. E. Johns, and T. L. Townsend, Rings of the North Brazil Current: their structure and behavior inferred from observations and a numerical simulation, *J. Geophys. Res., 100*, 10,633-10,654, 1995.

Garzoli, S. L., The Atlantic North Equatorial Countercurrent: Models and observations, *J. Geophys. Res., 97*, 17,931-17,946, 1992.

Gordon, A. L., Interocean exchange of thermocline water, *J. Geophys. Res., 91*, 5037-5046, 1986.

Gu, D., and S. G. H. Philander, Interdecadal climate fluctuations that depend on exchanges between the tropics and extratropics, *Science, 275*, 805-807, 1997.

Johns, W. E., T. N. Lee, F. A. Schott, R. J. Zantopp, and R. H. Evans, The North Brazil Current retroflection: Seasonal structure and eddy variability, *J. Geophys. Res., 95*, 22,103-22,120, 1990.

Johns, W. E., T. N. Lee, R. C. Beardsley, J. Candela, R. Limeburner, and B. Castro, Annual cycle and variability of the North Brazil Current, *J. Phys. Oceanogr., 28*, 103-128, 1998.

Katz, E. J., An interannual study of the Atlantic North Equatorial Countercurrent, *J. Phys. Oceanogr., 23*, 116-123, 1993.

Katz, E. J., R. L. Molinari, D. E. Cartwright, P. Hisard, H. U. Lass, and A. de Mesquita, The seasonal transport of the equatorial undercurrent in the western Atlantic (during the Global Weather Experiment), *Oceanol. Acta, 4*, 445-450, 1981.

Kennan, S. C., Observations of a tropical instability vortex, Ph.D. thesis, Univ. of Hawaii at Manoa, Honolulu, 1997.

Le Groupe CITHER 1, Recueil de données, Campagne CITHER 1, N.O. L'Atalante, Vol. 2/4; "CTDO2," *Rep. LPO 94-04,* 499 pp., Lab. de Phys. des Océans, IFREMER, Plouzané, France, 1994a.

Le Groupe CITHER 1, Recueil de données, Campagne CITHER 1, N.O. L'Atalante, Vol. 1/4; Mesures "en route," *Doc. Sci. O.P. 14*, 161 pp., Cent. ORSTOM, Cayenne, France, 1994b.

Le Groupe CITHER 2, Recueil de données, Campagne CITHER 2, N.O. Maurice Ewing, Vol. 2/4; "CTDO2," *Rep. LPO 95-04*, 521 pp., Lab. de Phys. des Océans, IFREMER, Plouzané, France, 1995.

Le Groupe CITHER 2, Recueil de données, Campagne CITHER 2, N.O. Maurice Ewing, Vol. 1/4; "Mesures en route," *Rep. LPO 96-01*, 179 pp., Lab. de Phys. des Océans, IFREMER, Plouzané, France, 1996.

L'Equipe ETAMBOT, Recueil de données, Campagne ETAMBOT 1, N.O. Le Noroit, Vol. 1/2; *Doc. Sci. O.P. 22,* 429 pp., Cent. ORSTOM, Cayenne, France, 1997a.

L'Equipe ETAMBOT, Recueil de données, Campagne ETAMBOT 2, N.O. Edwin Link, Vol. 1/2; *Doc. Sci. O.P. 24,* 521 pp., Cent. ORSTOM, Cayenne, France, 1997b.

Mayer, D. A., and R. H. Weisberg, A description of COADS surface meteorological fields and the implied Sverdrup transports for the Atlantic Ocean from 30°S to 60°N, *J. Phys. Oceanogr., 23*, 2201-2221, 1993.

Merle, J., and S. Arnault, Seasonal variability of the surface dynamic topography in the tropical Atlantic Ocean, *J. Mar. Res., 43*, 267-289, 1985.

Metcalf, W., Shallow currents along the northeastern coast of South America, *J. Mar. Res., 26*, 232-243, 1968.

Metcalf, W., and M. C. Stalcup, Origin of the Atlantic Equatorial Undercurrent, *J. Geophys. Res., 72*, 4959-4975, 1967.

Molinari, R. L., Observations of eastward currents in the tropical South Atlantic Ocean: 1978-1980, *J. Geophys. Res., 87*, 9707-9714, 1982.

Molinari, R. L., Observations of near-surface currents and temperature in the central and western tropical Atlantic Ocean, *J. Geophys. Res., 88*, 4433-4438, 1983.

Molinari, R. L., and E. Johns, Upper layer temperature structure of the western tropical Atlantic, *J. Geophys. Res., 99*, 18,225-18,233, 1994.

Pollard, R., and J. Read, A method for calibrating ship-mounted acoustic Doppler profilers, and the limitations of gyrocompasses, *J. Atmos. Oceanic Technol., 6*, 859-865, 1989.

Polonsky, A. B., E. G. Nikolaenko, S. Konate, and T. Camara, A study of the equatorial Atlantic currents using historical moored data, *Dt Sch. Hydrogr. Z., 45*, 219-254, 1993.

Reid, J. L., Jr., Evidence of a South Equatorial Counter Current in the Atlantic Ocean in July 1963, *Nature, 203*, 182, 1964.

Reverdin, G., P. Rual, Y. du Penhoat, and Y. Gouriou, Vertical structure of the seasonal cycle in the central equatorial Atlantic Ocean: XBT sections from 1980 to 1988, *J. Phys. Oceanogr., 21*, 277-291, 1991.

Richardson, P. L., and G. Reverdin, Seasonal cycle of velocity in the Atlantic north equatorial countercurrent as measured by surface drifters, current meters and shipdrifts, *J. Geophys. Res., 92*, 3691-3708, 1987.

Richardson, P. L., and D. Walsh, Mapping climatological seasonal variations of surface currents in the tropical Atlantic using ship drift data, *J. Geophys. Res., 91*, 10,537-10,550, 1986.

Richardson, P. L., G. Hufford, R. Limeburner, and W. S. Brown, North Brazil Current retroflection eddies, *J. Geophys. Res., 99*, 5081-5093, 1994.

Schmitz, W. J., Jr., On the interbasis-scale thermohaline circulation, *Rev. Geophys., 33*, 151-173, 1995.

Schmitz, W. J., Jr., and M. S. McCartney, On the North Atlantic circulation, *Rev. Geophys., 31*, 29-49, 1993.

Schmitz, W. J., Jr., and P. L. Richardson, On the source of the Florida current, *Deep Sea Res., Part A, 38*, suppl. 1, S379-S409, 1991.

Schott, F. A., and C. W. Böning, The WOCE model in the western equatorial Atlantic: Upper layer circulation, *J. Geophys. Res., 96*, 6993-7004, 1991.

Schott, F. A., J. Fischer, J. Reppin, and U. Send, On mean and seasonal currents and transport at the western boundary of the equatorial Atlantic, *J. Geophys. Res., 98*, 14,353-14,368, 1993.

Schott, F. A., L. Stramma, and J. Fischer, The warm water inflow into the western tropical Atlantic boundary regime, spring 1994, *J. Geophys. Res., 100*, 24,745-24,760, 1995.

Schott, F. A., J. Fischer, and L. Stramma, Transports and pathways of the upper-layer circulation in the western tropical Atlantic, *J. Phys. Oceanogr., 28*, 1904-1928, 1998.

Stramma, L., Geostrophic transport of the South Equatorial Current in the Atlantic, *J. Mar. Res., 49*, 281-294, 1991.

Stramma, L., and F. A. Schott, Western equatorial circulation and interhemispheric exchange, in *The Warmwatersphere of the North Atlantic Ocean*, edited by W. Krauss, pp.195-227, Gebrüder Borntræger, Berlin, 1996.

Stramma, L., J. Fischer, and J. Reppin, The North Brazil Undercurrent, *Deep Sea Res., Part I, 42*, 773-795, 1995.

Tsuchiya, M., Thermostads and circulation in the upper layer of the Atlantic Ocean, *Prog. Oceanogr., 16*, 235-267, 1986.

Wacongne, S., Dynamical regimes of a fully nonlinear stratified model of the Atlantic Equatorial Undercurrent, *J. Geophys. Res., 94*, 4801-4815, 1989.

Weisberg, R. H., and T. J. Weingartner, On the baroclinic response of the zonal pressure gradient in the equatorial Atlantic Ocean, *J. Geophys. Res., 91*, 11,717-11,725, 1986.

Weisberg, R. H., J. H. Hickman, T. Y. Tang, and T. J. Weingartner, Velocity and temperature observations during the seasonal response of the Equatorial Atlantic Experiment at 0°, 28°W, *J. Geophys. Res., 92*, 5061-5075, 1987.

Wilson, W. D., and W. E. Johns, Velocity structure and transport in the Windward Islands Passages, *Deep Sea Res., Part I, 44*, 487-520, 1997.

Wilson, W. D., E. Johns, and R. L. Molinari, Upper layer circulation in the western tropical North Atlantic Ocean during August 1989, *J. Geophys. Res., 99*, 22,513-22,523, 1994.

Worthington, L. V., On the North Atlantic circulation, *The Johns Hopkins Oceanogr. Stud., 6*, 110 pp., 1976.

B. Bourlès, Y. Gouriou, and R. Chuchla, Centre IRD de Bretagne, B.P. 70, 29280 Plouzané, France. (bourles@ird.fr; gouriou@ird.fr; chuchla@ird.fr)

(Received March 30, 1998; revised February 11, 1999; accepted February 25, 1999.)